Annu. Rev. Earth Planet. Sci. 2005. 33:531–70
doi: 10.1146/annurev.earth.33.092203.122614

First published online as a Review in Advance on February 1, 2005

THE Hf-W ISOTOPIC SYSTEM AND THE ORIGIN OF THE EARTH AND MOON

Stein B. Jacobsen
Department of Earth and Planetary Sciences, Harvard University, Cambridge, Massachusetts 02138; email: jacobsen@neodymium.harvard.edu

Key Words accretion, tungsten, isotopes, chronometer, core formation

■ **Abstract** The Earth has a radiogenic W-isotopic composition compared to chondrites, demonstrating that it formed while ^{182}Hf (half-life 9 Myr) was extant in Earth and decaying to ^{182}W. This implies that Earth underwent early and rapid accretion and core formation, with most of the accumulation occurring in ∼10 Myr, and concluding approximately 30 Myr after the origin of the Solar System. The Hf-W data for lunar samples can be reconciled with a major Moon-forming impact that terminated the terrestrial accretion process ∼30 Myr after the origin of the Solar System. The suggestion that the proto-Earth to impactor mass ratio was 7:3 and occurred during accretion is inconsistent with the W isotope data. The W isotope data is satisfactorily modeled with a Mars-sized impactor on proto-Earth (proto-Earth to impactor ratio of 9:1) to form the Moon at ∼30 Myr.

1. INTRODUCTION

The process of terrestrial planet-building probably began when a large population of small bodies (planetesimals) of roughly similar size coagulated into a smaller population of larger bodies. At early times, the size distribution of objects became skewed by runaway accretion toward a few large planetary embryos. These then accreted the smaller leftover bodies, and at some early time one of these embryos likely became dominant and could be identified as Earth. Toward the later stages of such a hierarchical accretion series, sweepup by Earth of the smaller embryos in its neighborhood led to giant collisions. The last collision could, in principle, have been of two ∼0.5 Earth mass bodies to form Earth, but is more commonly thought to have been with Earth and a 1–2 × Mars-sized body. The end result of this process was that at ∼1 AU only the Earth remained.

This review builds on the proposal by Jacobsen & Harper (1996) and Harper & Jacobsen (1996a) that the processes of planet formation and early differentiation (such as accretion, core formation, and early crust formation) are recorded in isotopic variations owing to the decay of extinct nuclides. The timescale of the accretion of the Earth could, therefore, be determined by making the correct isotopic

measurements of samples of meteorites and Earth. The ^{182}Hf-^{182}W system (9 Myr half-life) is clearly the most favorable chronometer of core formation during the planet-building processes as it directly tracks metal-silicate segregation. It is now well established that the silicate Earth exhibits a W isotopic composition that is more radiogenic than that of chondritic meteorites (Yin et al. 2002a,b; Schoenberg et al. 2002a; Kleine et al. 2002), demonstrating that the differentiation of Earth into a mantle and core occurred within the lifetime (∼30–50 Myr) of ^{182}Hf in the early Earth. Investigation of the ^{182}Hf-^{182}W system is also important in astrophysics because the initial abundance of ^{182}Hf in the Solar System provides a key constraint on models of the molecular cloud environment within which the Sun formed (Wasserburg et al. 1996). Hafnium-182 is predominantly an r-process radionuclide, but is also produced in the s-process under high neutron density conditions branching across unstable ^{181}Hf.

Metal segregation to form the core is now widely believed to have happened in an early terrestrial magma ocean, with final metal-silicate equilibration at very high P and T (Rubie et al. 2003). An early magma ocean also seems to be required to explain the noble gas signatures of the deep Earth (Harper & Jacobsen 1996b). This review presents a new and detailed description of the magma ocean differentiation model, originally developed for the Hf-W isotopic system by Harper & Jacobsen (1996a), which has become the most relevant model for interpreting Hf-W chronometry for Earth. Inferences drawn from all published Hf-W isotopic data using this model are reviewed in this paper, and it is also shown how this model can be directly linked to results from (*a*) experimental trace element partitioning and (*b*) computer simulations of the accretion process.

2. THE ^{182}Hf-^{182}W EXTINCT NUCLIDE SYSTEM

Hafnium-182 decays with a half-life of 9 Myr to ^{182}W. The isotopic composition of terrestrial W is given in Table 1. The Hf/W ratio of Earth is chondritic because Hf and W are highly refractory elements. The best estimate of the chondritic (CHUR = chondritic uniform reservoir) reference value for this ratio is $(\mathrm{Hf/W})_{CHUR} = 1.16$ for the atomic ratio corresponding to a Hf/W weight ratio of 1.123 (Harper & Jacobsen1996a). Hafnium is lithophile and is retained entirely in the silicate Earth during metal segregation. Tungsten, on the other hand, is moderately siderophile and is partitioned preferentially into the metal phase. Thus, the chondritic Hf/W

TABLE 1 The isotopic composition of tungsten (Jacobsen & Yin 1998)

	^{180}W	^{182}W	^{183}W	^{184}W	^{186}W
Abundance (%)	0.1194	26.498	14.313	30.641	28.428
^{i}W/^{183}W	0.00834 ± 4	1.85130 ± 4	≡1	≡2.14078	1.98613 ± 4
^{i}W/^{184}W	0.00390 ± 2	0.86478 ± 4	≡0.467119	≡1	0.92776 ± 2

ratio of Earth is internally fractionated by core formation. If core formation takes place during the lifetime of ^{182}Hf, an excess of ^{182}W should develop in the silicate Earth as a consequence of its enhanced Hf/W ratio. The W-isotope compositions of early metals will be deficient in ^{182}W relative to chondritic abundances because of the isolation of W before ^{182}Hf decayed. The Hf/W fractionation in reservoir j is defined relative to CHUR by $f^{Hf/W}$-values:

$$f_j^{Hf/W} = \frac{(^{180}Hf/^{183}W)_j}{(^{180}Hf/^{183}W)_{CHUR}} - 1, \tag{1}$$

where $(^{180}\mathrm{Hf}/^{183}\mathrm{W})_{CHUR} = 2.836$. Note that for the core or an iron meteorite $f^{Hf/W} = -1$, whereas for a silicate mantle of a differentiated planet $f^{Hf/W} > 1$ owing to partitioning of W into its core. Here $f^{Hf/W}$ is defined in terms of stable isotopes because ^{182}Hf is now extinct (see Equation 5 below).

The isotopic evolution of $^{182}\mathrm{W}/^{183}\mathrm{W}$ in a reservoir j today that evolved as a closed system is related to its initial composition at T_i by the standard geochronometry equation:

$$\left(\frac{^{182}W}{^{183}W}\right)_j^0 = \left(\frac{^{182}W}{^{183}W}\right)_j^{T_i} + \left(\frac{^{182}Hf}{^{183}W}\right)_j^0 (e^{\lambda t} - 1), \tag{2}$$

where the superscript 0 refers to the present value, T_i is some age close to the origin of the Solar System, and $\lambda = 0.077$ Myr^{-1} is the decay constant of ^{182}Hf. Here, the time t runs forward from the initial state at the formation of Earth. The time measured backward from today (i.e., the age) is called T, such that $T = T_0 - t$, where T_0 is the age of the Solar System today (as well as the maximum value of t). The best estimate of T_0 is 4567 Myr (Amelin et al. 2002).

Because of the short half-life of ^{182}Hf, this form of Equation 2 is not useful [for long times $(^{182}\mathrm{Hf}/^{183}\mathrm{W}) \sim 0$, $e^{\lambda t} \sim \infty$], and we rearrange it by introducing the following:

$$\left(\frac{^{182}Hf}{^{180}Hf}\right)_j^0 = \left(\frac{^{182}Hf}{^{180}Hf}\right)_{T_i} e^{-\lambda t}. \tag{3}$$

The W isotope evolution equation can thus be written in terms of readily measurable parameters:

$$\left(\frac{^{182}W}{^{183}W}\right)_j^0 = \left(\frac{^{182}W}{^{183}W}\right)_j^{T_i} + \left(\frac{^{182}Hf}{^{180}Hf}\right)_{T_i} \left(\frac{^{180}Hf}{^{183}W}\right)_j^0 (1 - e^{-\lambda t}). \tag{4}$$

At present, $e^{-\lambda t} \sim 0$, the system is extinct, and

$$\left(\frac{^{182}W}{^{183}W}\right)_j^0 = \left(\frac{^{182}W}{^{183}W}\right)_j^{T_i} + \left(\frac{^{182}Hf}{^{180}Hf}\right)_{T_i} \left(\frac{^{180}Hf}{^{183}W}\right)_j^0. \tag{5}$$

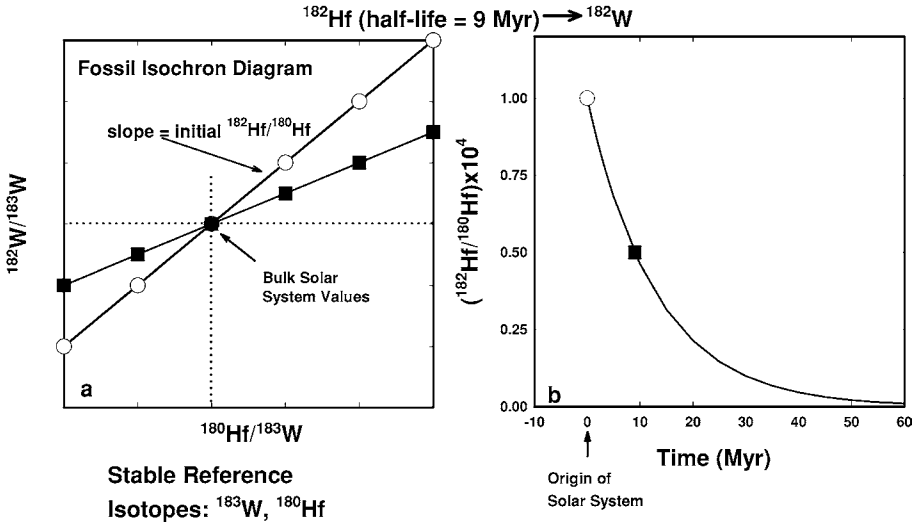

Figure 1 The ^{182}Hf-^{182}W chronometer. The slope of a line for a set of closed systems starting with the same initial $^{182}W/^{183}W$ in the fossil isochron diagram on the left yields the initial $^{182}Hf/^{180}Hf$ ratio of these closed systems. The ^{182}Hf decay curve shown on the right yields the times of formation and/or equilibration of systems that formed at different times subsequent to the formation of the Solar System. Examples are shown for a set of closed systems that formed at the time of formation of the Solar System (*open circles*) as well as one ^{182}Hf half-life (9 Myr) later.

In a plot of $^{182}W/^{183}W$ versus $^{180}Hf/^{183}W$, a fossil isochron diagram, the slope yields the initial $^{182}Hf/^{180}Hf$ value at T_i. This is shown schematically in Figure 1. From the data of Yin et al. (2002a,b) and Kleine et al. (2002), in Figure 2 we obtain the initial solar $^{182}Hf/^{180}Hf$ value at $T_i = T_0$ of $(^{182}Hf/^{180}Hf)_{T_0} = (1.0 \pm 0.1) \times 10^{-4}$ (see also Section 3.3, below). The initial solar W isotope ratio, $(^{182}W/^{183}W)^{T_0}_{CHUR} = 1.850664 \pm 37$, is given by the intercept of this isochron. Time differences based on fossil isochrons can thus be determined from Equation 3 as follows:

$$t = T_0 - T_i = -\frac{1}{\lambda} \ln \left[\frac{\left(\frac{^{182}Hf}{^{180}Hf}\right)_{T_i}}{\left(\frac{^{182}Hf}{^{180}Hf}\right)_{T_0}} \right]. \quad (6)$$

The evolution of $^{182}W/^{183}W$ from the inital solar value is shown schematically in Figure 3*a*, for both a chondritic reservoir (with $^{180}Hf/^{183}W = 2.836$) and a reservoir with a $^{180}Hf/^{183}W$ ratio of the bulk silicate Earth (BSE). The total enrichment in $^{182}W/^{183}W$ in such a reservoir over the history of the Solar System is $\approx 6.4 \cdot 10^{-4}$.

The W isotope composition of a sample or a reservoir *j* is often expressed as ε-deviations from the BSE:

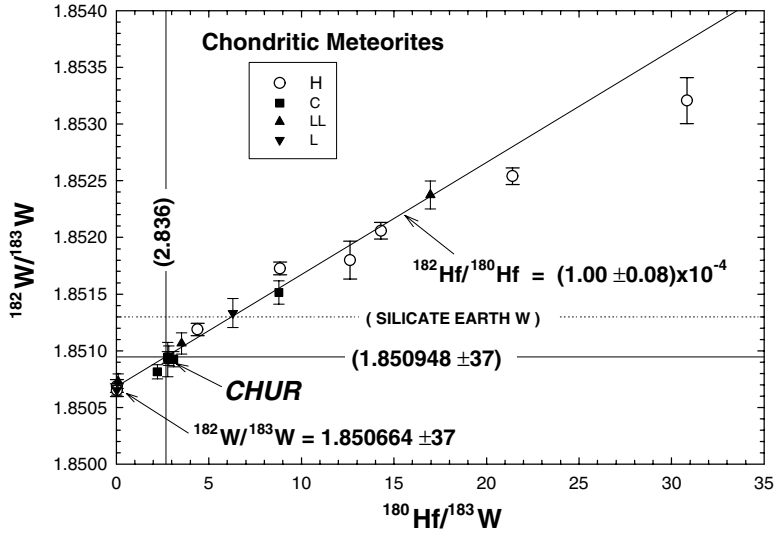

Figure 2 C, L, and LL chondrite data from Yin et al. (2002a,b) and H-chondrite data from Kleine et al. (2002).

$$\varepsilon_{W(BSE)j}(0) = \left[\frac{(^{182}W/^{183}W)^0_j}{(^{182}W/^{183}W)^0_{BSE}} - 1 \right] \times 10^4, \tag{7}$$

where $(^{182}\mathrm{W}/^{183}\mathrm{W})_{BSE} = 1.85130$ is based on a precisely determined laboratory W isotope standard that represents the silicate Earth. For W isotopes, any available terrestrial standard should be representative of the BSE composition. As shown in Figure 3*b*, the total enrichment of $^{182}\mathrm{W}/^{183}\mathrm{W}$ in such a reservoir over the history of the Solar System is ≈3.45 ε-units. In practice, both ^{183}W and ^{184}W have been used as reference isotopes (Table 1), but the ε_W notation means that this is of no consequence.

Using Equations 4 and 6 we have to very good approximation that

$$\varepsilon_{W(BSE)j}(0) \cong \varepsilon^I_{W(BSE)} + \left(\frac{^{182}Hf}{^{180}Hf} \right)_{T_0} q_W f_j^{Hf/W} (1 - e^{-\lambda t}), \tag{8}$$

where the intercept is

$$\varepsilon^I_{W(BSE)} \cong \varepsilon^{T_i}_{W(BSE)j} + \left(\frac{^{182}Hf}{^{180}Hf} \right)_{T_0} q_W (1 - e^{-\lambda t}), \tag{9}$$

and $q_W = 10^4(^{180}\mathrm{Hf}/^{182}\mathrm{W})^0_{CHUR} = 1.55 \times 10^4$. The size of the isotopic effects depend on the $f^{Hf/W}$ value (=12 for the BSE; see Table 2), the initial $^{182}\mathrm{Hf}/^{180}\mathrm{Hf}$, and q_W (see Figure 3*b*).

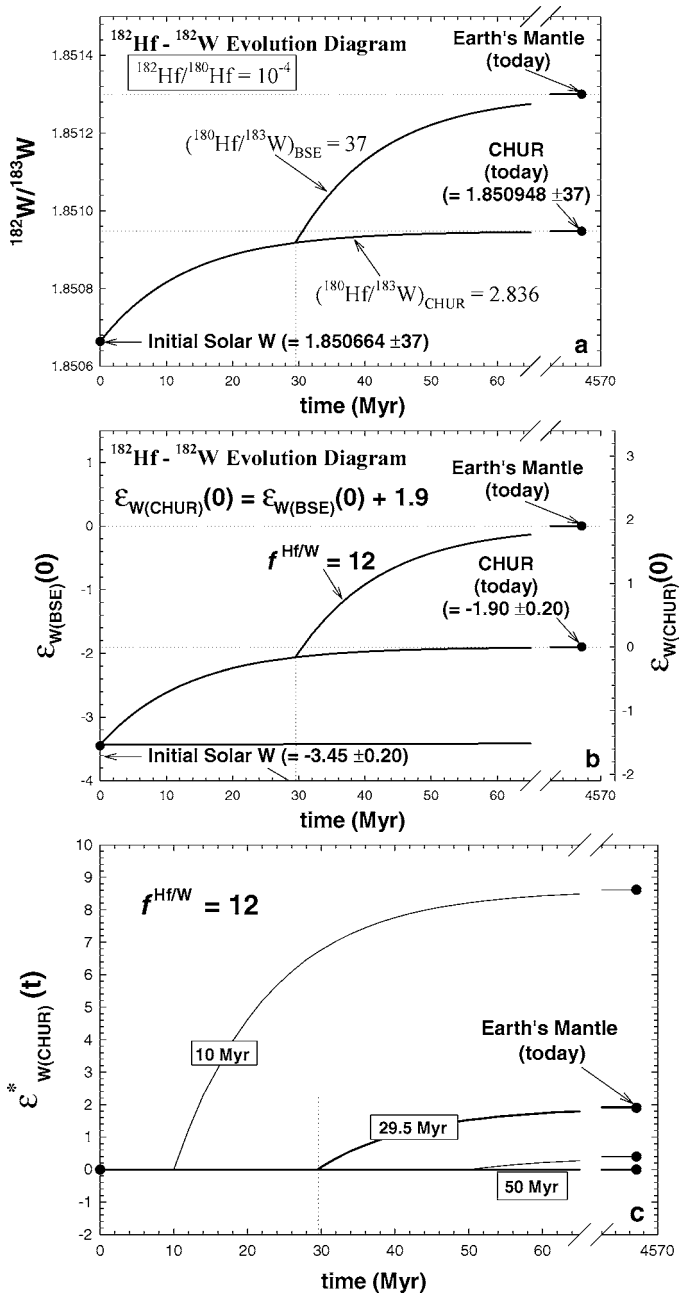

For calculation of model ages, referencing $^{182}W/^{183}W$ values to CHUR is necessary. The CHUR-normalized ε-unit notation is defined for a sample or reservoir j by

$$\varepsilon_{W(CHUR)j}(0) = \left[\frac{(^{182}W/^{183}W)^0_j}{(^{182}W/^{183}W)^0_{CHUR}} - 1 \right] \times 10^4$$
$$= \varepsilon_{W(BSE)j}(0) + 1.9, \quad (10)$$

where $(^{182}W/^{183}W)^0_{CHUR} = 1.850948$, and thus shows a simple relationship to the BSE normalized ε-values (see Figure 3*b*). The CHUR composition is measurable from chondrite measurements and is constrained to lie somewhere between iron meteorites and the composition of the BSE (see Figure 2 and Section 3.2, below).

The simplest model of fractionation is a two-stage model with a single episode of core-forming fractionation at an age T_{cf} occurring sometime after the origin of the Solar System at $T_0 = 4567$ Myr. In this case, we need the ε_W-value calculated relative to the chondritic evolution:

$$\varepsilon^*_{W(CHUR)j}(t) = \left[\frac{(^{182}W/^{183}W)^t_j}{(^{182}W/^{183}W)^t_{CHUR}} - 1 \right] \times 10^4, \quad (11)$$

where the time evolution of chondritic W $[(^{182}W/^{183}W)^t_{CHUR}]$ is obtained from Equation 4. The first stage of isotopic evolution is that of an unfractionated reservoir with $\varepsilon^*_{W(CHUR)_j}(t) = 0$. Isotopic evolution relative to CHUR occurs only in the second stage after fractionation to form the core at time $t_{2stage} = T_0 - T_{cf}$. The isotopic time evolution of j for $t \geq t_{2stage}$ is given by

$$\varepsilon^*_{W(CHUR)j}(t) = q_W \left(\frac{^{182}Hf}{^{180}Hf} \right)_{T_0} f_j^{Hf/W} [e^{-\lambda t_{2stage}} - e^{-\lambda t}]. \quad (12)$$

A plot of the $\varepsilon_{W(CHUR)}$ evolution for the BSE ($f^{Hf/W} = 12$) versus the time, assuming core formation ($T_0 - T_{cf}$) at 10, 29.5, and 50 Myrs is shown in Figure 3*c*. As shown, subsequent to 50 Myrs, there is insignificant ε_W evolution.

←

Figure 3 Various plots of early Solar System ^{182}Hf-^{182}W evolution in planetary reservoirs and three different types of ε_W-values: (*a*) Schematic showing the $^{182}W/^{183}W$ evolution including fractionation of Hf from W in Earth mantle. (*b*) Same diagram with present ε_W values relative to the bulk silicate earth (BSE) and *f*-notation. Earth's mantle (BSE) has $f^{Hf/W} = 12$. The relationship between present ε_W-values relative to BSE and ε_W relative to average chondrites (CHUR) is also given. (*c*) Same diagram as above but with ε_W-values relative to the chondritic evolution of $^{182}W/^{183}W$. As shown, subsequent to ~50 Myr after the origin of the Solar System it is hard to generate substantial W-isotopic variations.

TABLE 2 The isotopic composition of tungsten and chemical fractionations of various planetary mantles and cores

	Mantle $\varepsilon_{W(BSE)}$ **(0)**	**Mantle** $\varepsilon_{W(CHUR)}$ **(0)**	**Core** $\varepsilon_{W(BSE)}$ **(0)**	**Core** $\varepsilon_{W(CHUR)}$ **(0)**	**Mantle** $f^{Hf/W}$	t_{2stage} **(Myr)**	**Core mass fraction** (γ)	$D_W^{met/sil}$
Earth	*≡0*	1.9 ± 0.2	-2.06 ± 0.05	-0.16 ± 0.05	*12 ± 2*	29.6	*0.325*	24.9
Moon	*1.3 ± 0.4*	3.2 ± 0.4	-2.08 ± 0.05	-0.18 ± 0.05	*18 ± 2*	28.1	*<0.02, 0.325*	>882, 37
IAB	19.1	21	*−3.30 ± 0.15*	-1.40 ± 0.15	(15)	<2.8	*0.2*	60
IIAB	22.1	24	*−3.50 ± 0.36*	-1.60 ± 0.36	(15)	<2.9	*0.2*	60
IIIAB	29.5	31.4	*−3.99 ± 0.60*	-2.09 ± 0.60	(15)	<0.5	*0.2*	60
IVA	30.8	32.7	*−4.08 ± 0.69*	-2.18 ± 0.69	(15)	<0.5	*0.2*	60
IVB	29.2	31.1	*−3.97 ± 0.42*	-2.07 ± 0.42	(15)	∼0	*0.06*	235
Vesta	*17 ± 2*	19 ± 2	-3.17 ± 0.34	-1.27 ± 0.34	*15 ± 2*	2.6	*0.2*	60
Mars—S source	*0.5 ± 0.5*	2.4 ± 0.5	-3.10 ± 0.52	-1.20 ± 0.52	*2.0 ± 0.8*	3.3	*0.2*	8
Mars—NC source	*2.5 ± 0.5*	4.4 ± 0.5	-2.63 ± 0.25	-0.73 ± 0.25	*6 ± 1*	9.7	*0.2*	24

Values in italics are primary data (see text for sources), other values are inferred from these. Numbers in parentheses are best guesses.

For $t = T_0$ we obtain the present effect:

$$\varepsilon_{W(CHUR)j}(0) = q_W \left(\frac{^{182}Hf}{^{180}Hf}\right)_{T_0} f_j^{Hf/W} e^{-\lambda t_{2stage}}, \tag{13}$$

where $t_{2stage} = (T_0 - T_{cf})$. Thus the time of differentiation for a two-stage model is

$$t_{2stage} = \frac{1}{\lambda} \ln \left[\frac{q_W \left(\frac{^{182}Hf}{^{180}Hf}\right)_{T_0} f_j^{Hf/W}}{\varepsilon_{W(CHUR)_j(0)}} \right]. \tag{14}$$

With a $\varepsilon_{W(CHUR)}$ of +1.9 in the BSE, we obtain a time of core formation $(T_0 - T_{cf})$ of 29.5 Myr (see Table 2).

An equivalent method is to calculate t_{2stage} directly from isotope ratios:

$$t_{2stage} = \frac{1}{\lambda} \ln \left[\frac{\left(\frac{^{182}Hf}{^{180}Hf}\right)_{T_0} \left[\left(\frac{^{180}Hf}{^{183}W}\right)_j - \left(\frac{^{180}Hf}{^{183}W}\right)_{CHUR} \right]}{\left(\frac{^{182}W}{^{183}W}\right)_j^0 - \left(\frac{^{182}W}{^{183}W}\right)_{CHUR}^0} \right]. \tag{15}$$

Also note that for a reservoir that formed at T_0 with no Hf ($f^{Hf/W} = 0$), we have

$$\varepsilon_{W(CHUR)j}(0) = -q_W \left(\frac{^{182}Hf}{^{180}Hf}\right)_{T_0} = -1.55. \tag{16}$$

3. TUNGSTEN ISOTOPE MEASUREMENTS

Hf-W isotopic data that constrain the evolution of planetary mantles and cores are reviewed below and summarized in Table 2. This table gives the core mass fractions (γ) for Earth and Mars (cf. Taylor 1992), the Moon (Stegman et al. 2003), the IAB, IIAB, IIIAB, IVA and IVB iron meteorite parent bodies (Petaev & Jacobsen 2004), and Vesta (Ruzicka et al. 1997, Righter & Shearer 2003). The measured $\varepsilon_{W(BSE)}(0)$-values in this table are converted to $\varepsilon_{W(CHUR)}(0)$ (using Equation 10) and given in a separate column in Table 2 because the $\varepsilon_{W(BSE)}(0)$-values relative to CHUR are required for model calculations.

3.1. Earth

The silicate Earth has a high Hf/W ratio corresponding to $f^{Hf/W} = 12 \pm 2$ owing to partitioning of most of Earth's W into the core (Harper & Jacobsen 1996a, Halliday et al. 2000, Halliday 2004). The results described for chondrites below mean that the BSE has a radiogenic $^{182}W/^{183}W$ signature of $\varepsilon_{W(CHUR)}(0) = 1.9 \pm 0.2$. This yields $t_{2stage} = 29.5$ Myr, which would be the time of formation of the core if the whole core segregated from the mantle at this time. No variations have been

found in either young or old terrestrial samples (Yin et al. 1999; Schoenberg et al. 2002a,b; Schersten et al. 2004) except possibly for a few samples from Isua, western Greenland that appear to have low $^{182}W/^{183}W$ ratios owing to a meteorite component (Schoenberg et al. 2002b).

3.2. The Initial Solar $^{182}W/^{183}W$ Isotope Ratio and Iron Meteorite Parent Bodies

Tungsten from large samples of the Toluca iron meteorite with a Hf/W = 0 were initially used as a proxy of the initial Solar System $^{182}W/^{183}W$ composition (Harper et al. 1991). The first well-resolved effect of $\varepsilon_{W(BSE)}(0) = -3.9 \pm 1.0$ was reported by Harper & Jacobsen (1994a,b; 1996a) and Jacobsen & Harper (1996). Jacobsen & Yin (1998) reported an improved result of $\varepsilon_{W(BSE)}(0) = -3.3 \pm 0.1$ for the Toluca meteorite. Similar results were reported for other iron metorites by Lee & Halliday (1995, 1996). Horan et al. (1998) reported the currently most complete study of iron meteorite groups, and their average values for each group are listed in Table 2. The initial $\varepsilon_{W(BSE)}(0)$ we have obtained on metals from chondrites is -3.45 ± 0.25 (see section below), and is likely close to the initial solar value. Quitte & Birck (2004) recently proposed a lower value of -4.4 ± 0.4 for the inital value based on the measurement of a single IVB meteorite, Tlacotepec. In the same study, they revised the $\varepsilon_{W(BSE)}(0)$-value of the IVA meteorite Duel Hill from -5.0 ± 1.0 to -3.5 ± 0.3. Yin & Jacobsen (2003) also reported additional iron meteorite results and could not find any values significantly below the -3.45 ± 0.25 value from the chondrite isochron. At this stage, it is premature to revise the initial solar values based on this new single measurement of Tlacotepec. Clearly, more precise $\varepsilon_{W(BSE)}(0)$ data on iron meteorites are needed before this issue is settled. Another parameter of significance for Hf-W chronometry of iron meteorite parent bodies is the $f^{Hf/W}$-value of their silicate mantles. Because it is an unknown value, we have assumed $f^{Hf/W} = 15$ based on analogy with another differentiated planetesimal, Vesta. Using such a $f^{Hf/W}$-value would yield a range of t_{2stage} from $\sim$0 to $<$2.8 Myr.

3.3. Chondritic Hf-W Parameters and the Initial Solar $^{182}Hf/^{180}Hf$

The first report of the W isotope composition of chondrites was by Lee & Halliday (1995, 1996). They concluded that it was identical to terrestrial W. However, recently, three groups reported that $^{182}W/^{183}W$ in chondrites is lower than that of Earth by $\sim$2 ε_W-units, and thus intermediate between the initial solar $^{182}W/^{183}W$ and that of Earth today (Yin et al. 2002a,b; Schoenberg et al. 2002a; Kleine et al. 2002). These new results supersede previous chondrite data (Lee & Halliday 1995; 1996; 2000a,b) and have fundamentally changed the way in which the Hf-W chronometer can be used because they demonstrate that ^{182}Hf was live when Earth formed. Figure 2 shows that the data of Yin et al. (2002a,b) for the ordinary chondrites Dalgety Downs and Dhurmsala yield a well-defined fossil

isochron array. Four separate whole-rock samples of carbonaceous chondrites (three Allende and one Murchison) as well as a calcium-aluminum-rich inclusion (CAI) from the Allende meteorite are plotted on this isochron. The fact that a CAI from the Allende meteorite plots within error of this isochron requires the Hf-W age of these ordinary chondrites to be roughly similar to (within ~1 Myr) the age of the oldest solid objects of the Solar System (Allende CAIs). The combined chondrite isochron gives an initial $^{182}Hf/^{180}Hf = 1.00 \pm 0.08 \times 10^{-4}$ and an initial $^{182}W/^{183}W$ ratio corresponding to $\varepsilon_W = -3.45 \pm 0.25$. Most of the H-chondrite data (Forest Vale and St. Margurite) of Kleine et al. (2002) also plot on this isochron, except for the two highest points from St. Marguerite. Kleine et al. (2002) argued that the Pb-Pb age of the phosphate in St. Marguerite could be used to correct for the effect of metamorphism in this meteorite. By this approach they obtained an initial $^{182}Hf/^{180}Hf = 1.09 \pm 0.09 \times 10^{-4}$ within error of the reference isochron in Figure 2. This new initial $^{182}Hf/^{180}Hf$ value of $1.00 \pm 0.08 \times 10^{-4}$ is significantly lower and clearly inconsistent with the previously used value of 2.75×10^{-4} (Lee & Halliday 2000a). As shown in Figure 2 the bulk chondrite values on this fossil isochron are consistent with a CHUR value of $\varepsilon_{W(BSE)} = -1.9 \pm 0.2$ and $f^{Hf/W} = 0$ and a initial solar $^{182}Hf/^{180}Hf$ of $1.00 \pm 0.08 \times 10^{-4}$.

3.4. Moon

The La/W ratio of the Moon (Rammensee & Wänke 1977) was used to obtain $f^{Hf/W} = 18 \pm 2$. The initial report of W isotope variations in lunar samples (Lee et al. 1997) required the Moon to have a substantially higher $\varepsilon_{W(BSE)}$-value than Earth (average of +2–3; range of ~0 to +7). It is now apparent that a significant portion of the observed $\varepsilon_{W(BSE)}$ variation in these lunar samples was not due to ^{182}Hf decay, but instead related to the reaction ^{181}Ta (n,γ) ^{182}Ta (β^-) ^{182}W induced by cosmic ray bombardment while these rocks were exposed on the surface of the Moon (Lee et al. 2002). The residual radiogenic ^{182}W signature from ^{182}Hf decay for the Moon is now estimated at $\varepsilon_{W(BSE)} = 1.3 \pm 0.4$ based on the lunar KREEP basalt 15555 (Lee et al. 2002). Together with the Moon's $f^{Hf/W}$-value, this yields a two-stage model time of $t_{2stage} = 28.1$ Myr. For the Moon, such model time may be a good estimate of its time of formation because it may satisfy the basic assumption that it formed with $\varepsilon_{W(CHUR)} \sim 0$ (see Section 5) and thereafter evolved as a closed system. There is still substantial uncertainty associated with interpretation of cosmogenic ^{182}W effects in lunar samples (Yin et al. 2003).

3.5. Eucrites and Vesta

The mantle of the eucrite parent body (probably the asteroid Vesta) shows a clear signature of core formation based on La/W-ratios in eucrite meteorites (Palme & Rammensee 1981). The La/W ratio in these meteorites yields an estimate of $f^{Hf/W} \approx 15 \pm 2$ for the eucrite parent body mantle (Yin et al. 2002b). Such a high Hf/W reservoir would be expected to have a radiogenic ^{182}W signature, and

this was found in the first Hf-W isotopic study of eucrites by Lee & Halliday (1997). Later, Quitté et al. (2000) reported a Hf-W fossil isochron with a high initial $\varepsilon_{W(BSE)}$ of ~ -1 and an initial $^{182}Hf/^{180}Hf = 7.96 \times 10^{-5}$. The Juvinas (eucrite) measurement of Yin et al. (2002b) is consistent with this eucrite isochron. Quitté et al. (2000) compared their result to the then accepted high initial solar $^{182}Hf/^{180}Hf$ value of 2.75×10^{-4} (Lee & Halliday 1995, 1996, 2000a), which indicated a late parent body (Vesta) differentiation at $\sim$16 Myr. However, using the now accepted $^{182}Hf/^{180}Hf$ value of 1.0×10^{-4} suggests that the eucrites postdate ordinary chondrites by only $\sim$3 Myr. This is consistent with the evidence for live ^{53}Mn ($t_{1/2} = 3.7$ Myr; Lugmair & Shukolyukov 1998) and ^{26}Al ($t_{1/2} = 0.7$ Myr; Srinivasan et al. 2000, Nyquist et al. 2001) in eucrites because ^{53}Mn and ^{26}Al chronologies also indicate that the eucrites formed at $\sim$3 Myr. From the eucrite isochron (Quitté et al. 2000), the Vesta mantle should have a present-day $\varepsilon_{W_{(BSE)}} \sim +17 \pm 2$, which, together with the $f^{Hf/W}$-value of the mantle, yields $t_{2stage} = 2.6$ Myr for Vesta's mantle.

3.6. Mars

Lee & Halliday (1997) found that the shergottite-nakhlite-chassignite (SNC) meteorites (martian meteorites) exhibit a range in $\varepsilon_{W(BSE)}(0)$ from approximately $+0.5 \pm 0.5$ for the shergottite (S) meteorites to much higher values of $+2$ to $+3$ for the NC (nakhlite-chassignite) meteorites. New data from Foley et al. (2003, 2004) support these results. Lee & Halliday (1997) also suggested a correlation with ε_{142Nd}-values reported by Harper et al. (1995) for the same meteorites. However, the new data by Foley et al. (2004) does not support such a correlation. Instead it looks like the S mantle source exhibits relatively uniform $\varepsilon_{W(BSE)}(0)$-values of 0.5 ± 0.5, but variable ε_{142Nd} ranging from $\sim$0 to 1.0, whereas the NC mantle source exhibits both high $\varepsilon_{W(BSE)}(0)$ of 2.5 ± 0.5 as well as high ε_{142Nd} of 0.5 to 1.0. These sources also appear to have distinct $f^{Hf/W}$-values of 2.0 ± 0.8 for the S source (Righter & Drake 1996, Treiman et al. 1986) and 6 ± 1 for the NC source [based on compilation by Lodders (1998)]. This yields t_{2stage} model times of 3.3 and 9.7 Myr for the S and NC sources, respectively.

4. MODELING OF METAL-SILICATE SEPARATION IN THE TERRESTRIAL PLANETS

Radio-nuclides and trace elements, together with transport models for the accretion and core-formation processes, provide powerful tools for investigating timescales associated with planetary accretion. The purpose here is to derive solutions to the governing equations for transport of mass and species for the magma ocean model of Harper & Jacobsen (1996a), such that it can be used to (*a*) interpret data for both short-lived (^{182}Hf-^{182}W, ^{107}Pd-^{107}Ag, etc.) and long-lived (^{238}U-^{206}Pb, etc.) radiogenic isotope systems, (*b*) provide a direct link to experimentally determined metal-silicate partitioning data, and (*c*) provide a direct connection to astrophysical

models of planetary accretion. The principles and notation follow those outlined by Jacobsen (1988) and Jacobsen & Wasserburg (1979).

The mean age of the mass of a reservoir of interest (j) was introduced by Jacobsen & Wasserburg (1979) for the relationship between radionuclide signatures and the rates of mass transfer between planetary reservoirs. It is useful for understanding chronologies of continuous processes because it can be simply related to the different forms of the rate function or cumulative mass growth curve for a reservoir. For a growing reservoir with no significant losses, the mean age after a time t is given by

$$\langle T_j(t)\rangle = \frac{1}{M_j(t)} \int_0^t M_j(\xi)\, d\xi. \tag{17}$$

It has a very simple relation to isotopic signatures for long-lived decay systems if the chemical fractionation factor of the parent/daughter elemental ratio remains constant during the process (Jacobsen & Wasserburg 1979). Jacobsen & Harper (1996) showed that a different, but simple, set of relationships between extinct isotope signatures and mean ages also exist. For extinct nuclides, it is usually more convenient to use the mean time of formation $\langle t_j\rangle$ because the mean age is usually close to the value of T_0:

$$\langle t_j\rangle = T_0 - \langle T_j(t)\rangle. \tag{18}$$

The model is based on isotopic and chemical mass balance between a primitive solar nebular reservoir, the primitive mantle, and the core. This allows us to evaluate transport and chemical fractionation specifically associated with metal-silicate separation owing to core formation from observed isotopic variations.

4.1. Evolution of Mass During Accretion and Core Formation

The growth of Earth is considered to be from a primitive solar nebular reservoir (reservoir 1)—this is simply all the solar nebular material that ends up in Earth. The model is shown schematically in Figure 4. As Earth grows it is continuously differentiated into two reservoirs: a silicate mantle (reservoir 2) and a metal core (reservoir 3) owing to metal segregation in the mantle. The newly accreted material is assumed to mix with the silicate Earth before segregating new core material in a magma ocean (see Jacobsen et al. 2004 and manuscript in preparation as well as Section 6.3). We define M_j to be the total mass of reservoir j, and thus, by mass balance,

$$M_1(0) = M_1(t) + M_2(t) + M_3(t). \tag{19}$$

The rate of growth of Earth (the mass accretion rate) is

$$\frac{dM_\oplus}{dt} = \dot{M}_{accr}, \tag{20}$$

and the mass of Earth ($M_\oplus$) as a function of time is

$$M_\oplus(t) = \int_0^t \dot{M}_{accr}(\xi)\, d\xi = M_3(t) + M_2(t) = M_1(0) - M_1(t). \qquad (21)$$

If $\dot{M}_{jk}$ is the mass flux from reservoir j to k, then the rate of change of the mass of the primitive nebular reservoir is

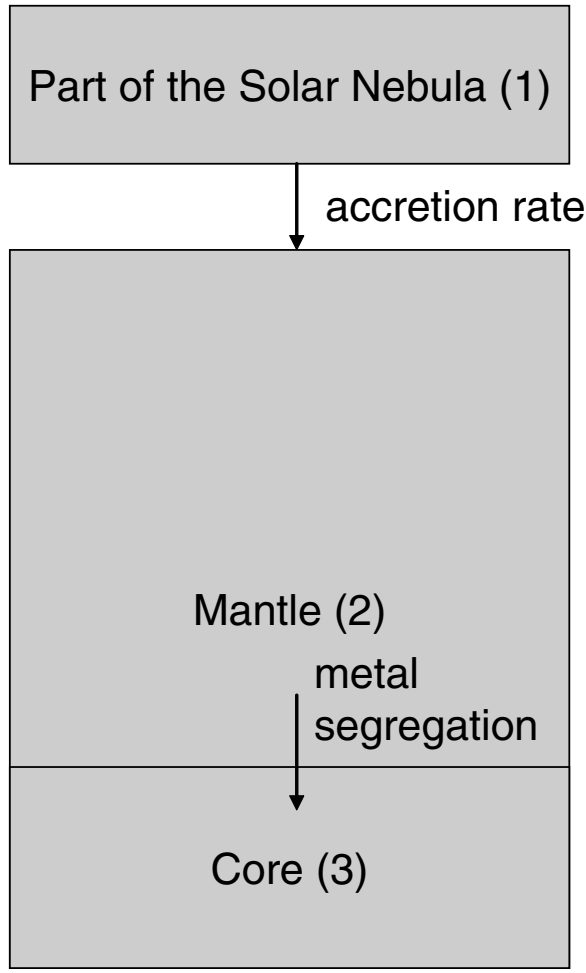

Figure 4 Cartoon illustrating the continuous core formation model with metal segregation in a magma ocean. Earth is assumed to accrete from material with a chondritic in Hf/W ratio and a chondritic W-isotopic composition. Newly segregated core material is assumed to reflect the average isotopic composition of the magma ocean.

$$\frac{dM_1}{dt} = -\dot{M}_{12} = -\dot{M}_{accr}. \tag{22}$$

This assumes $\dot{M}_{13} = 0$, and cases with $\dot{M}_{13} > 0$ are discussed in a separate paper (Jacobsen et al. 2004 and manuscript in preparation).

If the fraction of core forming at any time is $\gamma = \dot{M}_{23}/\dot{M}_{12}$, then the rates of change of the mass of the mantle and core and are

$$\frac{dM_2}{dt} = \dot{M}_{12} - \dot{M}_{23} = (1-\gamma)\dot{M}_{12} = (1-\gamma)\dot{M}_{accr} \tag{23}$$

$$\frac{dM_3}{dt} = \dot{M}_{23} = \gamma\dot{M}_{12} = \gamma\dot{M}_{accr}. \tag{24}$$

Integrating we obtain the following:

$$M_2(t) = M_{\oplus}(t) - \int_0^t \gamma\dot{M}_{accr}(\xi)\,d\xi \tag{25}$$

$$M_3(t) = \int_0^t \gamma\dot{M}_{accr}(\xi)\,d\xi. \tag{26}$$

In the case that γ is constant,

$$M_2(t) = (1-\gamma)\int_0^t \dot{M}_{accr}(\xi)\,d\xi = (1-\gamma)M_{\oplus}(t) \tag{27}$$

$$M_3(t) = \gamma\int_0^t \dot{M}_{accr}(\xi)\,d\xi = \gamma M_{\oplus}(t). \tag{28}$$

In such a model, the average age of Earth is the same as the average age of the core and mantle.

4.2. The Primitive Solar Nebular Source Reservoir for Earth

The composition of this reservoir is constant except for variations owing to radioactive decay or production. We define N_{ij} and C_{ij} $(= N_{ij}/M_j)$ to be the number of atoms of species i in reservoir j and the concentration of species i in reservoir j, respectively. We consider four different types of species: (i) radioactive species r (such as ^{182}Hf), (ii) radioactive daughter products d (such as ^{182}W), and (iii) two types of stable species: ρ is of the same element as r (normally ^{180}Hf if $r = {}^{182}$Hf) and s is of the same element as d (normally ^{183}W if $d = {}^{182}$W). The concentrations of each of these species in reservoir 1 are simply

$$C_{s1}(t) = C_{s1}(0) \tag{29}$$

$$C_{\rho 1}(t) = C_{\rho 1}(0) \tag{30}$$

$$C_{r1}(t) = C_{r1}(0)e^{-\lambda t} \tag{31}$$

$$C_{d1}(t) = C_{d1}(0) + C_{r1}(0)[1 - e^{-\lambda t}] \tag{32}$$

and their total inventories are

$$N_{i1}(t) = C_{i1}(t)\, M_1(t) \tag{33}$$

for $i = r$, ρ , d and s.

4.3. Transport of Stable Trace Species

If the flux of species i from reservoir j to k is J_{ijk}, then the transport equation for reservoir 1 for stable species (i = s, ρ) is

$$\frac{dN_{i1}}{dt} = -J_{i12} = -C_{i1}\dot{M}_{12}, \tag{34}$$

and the solution is

$$N_{i1}(t) = N_{i1}(0) - C_{i1}M_{\oplus}(t). \tag{35}$$

The concentrations in the mantle and the core are, however, affected by the metal-silicate enrichment factor ($i = r$, ρ, d and s):

$$d_{i23} = \frac{c_{i3}}{C_{i2}} = D_i^{metal/silicate}, \tag{36}$$

where c_{i3} is the concentration in a new addition to the core and $D_i^{metal/silicate}$ is the metal/silicate partition coefficient. The equality $d_{i23} = D_i^{metal/silicate}$ holds for chemical equilibrium between metal and silicate. If equilibrium is not achieved, then the treatment given here is still valid and d_{i23} is simply the effective chemical enrichment factor of an element in segregated metal relative to the silicate mantle. Because $\dot{M}_{23} = \gamma \dot{M}_{12}$, the equation for the mantle can be written as

$$\begin{aligned}
\frac{dN_{i2}}{dt} &= J_{i12} - J_{i23} = C_{i1}\dot{M}_{12} - d_{i23}C_{i2}\dot{M}_{23} \\
&= (C_{i1} - \gamma d_{i23}C_{i2})\,\dot{M}_{12} \\
&= \frac{\dot{M}_2}{1-\gamma}\left(C_{i1} - d_{i23}\gamma\frac{1}{M_2}N_{i2}\right) \\
&= \frac{C_{i1}\dot{M}_2}{1-\gamma} - \frac{\gamma d_{i23}}{1-\gamma}\frac{\dot{M}_2}{M_2}N_{i2}
\end{aligned} \tag{37}$$

for $i = s$, ρ and $\dot{M}_2 = dM_2/dt$. Integrating [assuming $N_{i2}(0) = 0$] yields the solution for a stable index isotope:

$$N_{i2}(t) = \frac{C_{i1}}{(d_{i23} - 1)\,\gamma + 1} M_2(t). \tag{38}$$

Thus, the concentration can be written as

$$\frac{C_{i2}}{C_{i1}} = \frac{1}{(d_{i23} - 1)\,\gamma + 1}. \tag{39}$$

This is equivalent to the expression for static models of trace element partitioning (cf. Righter & Drake 1997) used to compare high P, T partitioning data with $D_i^{metal/silicate}$-values estimated from the mantle's siderophile element pattern (cf. Righter & Drake 2000, Gessmann & Rubie 2000, Drake & Righter 2002, Rubie et al. 2003).

Once N_{i2} is known, the core can be calculated by mass balance:

$$\begin{aligned} N_{i3}(t) &= N_{i1}(0) - N_{i1}(t) - N_{i2}(t) \\ &= C_{i1} M_{\oplus}(t) - N_{i2}(t). \end{aligned} \tag{40}$$

Thus,

$$N_{i3}(t) = \left[\frac{d_{i23} C_{i1}}{(d_{i23} - 1)\,\gamma + 1} \right] M_3(t), \tag{41}$$

and the concentrations in the core are

$$\frac{C_{i3}}{C_{i1}} = \frac{d_{i23}}{(d_{i23} - 1)\,\gamma + 1}. \tag{42}$$

4.4. Transport of Radioactive Species

For a radioactive species (r) (such as ^{182}Hf or ^{238}U) we have the following:

$$\frac{dN_{r2}}{dt} = C_{r1}(0) e^{-\lambda t} \dot{M}_{12} - d_{r23} C_{r2} \dot{M}_{23} - \lambda N_{r2}, \tag{43}$$

which gives the following result for the mantle and core (reservoirs 2 and 3):

$$N_{r2}(t) = \frac{e^{-\lambda t} C_{r1}(0)}{(d_{r23} - 1)\,\gamma + 1} M_2(t) \tag{44}$$

$$N_{r3}(t) = \frac{e^{-\lambda t} d_{r23} C_{r1}(0)}{(d_{r23} - 1)\,\gamma + 1} M_3(t). \tag{45}$$

The chemical fractionation factors ($f^{r/s}$-values) of the ratio of a radioactive isotope to a stable isotope in a reservoir j relative to that in reservoir 1 is as usual defined by

$$f_j^{r/s} = \frac{\frac{N_{r,j}(t)}{N_{s,j}(t)}}{\frac{N_{r,1}(t)}{N_{s,1}(t)}} - 1. \tag{46}$$

For constant d- and γ-values, the $f^{r/s}$-values for reservoirs 2 and 3 are independent of time and given by

$$f_2^{r/s} = \frac{\gamma\,[d_{s23} - d_{r23}]}{(d_{r23} - 1)\,\gamma + 1} \tag{47}$$

$$f_3^{r/s} = \frac{[\gamma - 1]\,(d_{s23} - d_{r23})}{d_{s23}\,[(d_{r23} - 1)\,\gamma + 1]}. \tag{48}$$

Also note that $f_j^{\rho/s} = f_j^{r/s}$ because $d_{\rho 23} = d_{r23}$.

For the ^{182}Hf-^{182}W system, we obtain the following simple results (because Hf is not partitioned into the core, with $d_{r23} = 0$):

$$f_2^{\rho/s} = f_2^{r/s} = \frac{\gamma d_{s23}}{1 - \gamma} \quad \text{and} \quad f_3^{\rho/s} = f_3^{r/s} = -1. \tag{49}$$

Thus, for the Hf-W system, we can estimate the $d_{W23} = D_W^{metal/silicate}$-value from the $f_2^{Hf/W}$ and γ-values in Table 2. This yields a range of $D_W^{metal/silicate}$-values; however, there is no correlation with planet size as might be expected from the strong pressure dependence of this partition coefficient (Righter & Drake 1999, Walter et al. 2000, Righter & Shearer 2003). It is also a strong function of f_{O_2} and melt composition, which may obscure any relationship to planet size. Cases with D as a function of t are considered in a separate paper (Jacobsen et al. 2004 and manuscript in preparation).

4.5. The Transport and Evolution of Daughter Isotopes

Introducing $R_d = N_d/N_s$ (i.e., ^{182}W/^{183}W), we obtain

$$\frac{dR_{d2}}{dt} = \frac{1}{N_{s2}}\left[\left(\frac{dN_{d2}}{dt}\right) - R_{d2}\left(\frac{dN_{s2}}{dt}\right)\right]. \tag{50}$$

For a radiogenic isotope d (such as ^{182}W) the transport equation is ($d_{s23} = d_{d23}$)

$$\begin{aligned}\frac{dN_{d2}}{dt} &= J_{d12} - J_{d23} + \lambda N_{r2} = C_{d1}\dot{M}_{12} - d_{s23}C_{d2}\dot{M}_{23} + \lambda N_{r2} \\ &= (C_{d1} - d_{s23}\gamma C_{d2})\,\dot{M}_{12} + \lambda N_{r2}\end{aligned} \tag{51}$$

and

$$\frac{dR_{d2}}{dt} = \frac{1}{N_{s2}}\left[(C_{d1} - d_{s23}\gamma C_{d2})\,\dot{M}_{12} + \lambda N_{r2} - R_{d2}\left(\frac{dN_{s2}}{dt}\right)\right]. \tag{52}$$

Inserting the stable isotope equation,

$$\frac{dN_{s2}}{dt} = \dot{M}_{12}(C_{s1} - d_{s23}\gamma C_{s2}), \tag{53}$$

and $\dot{M}_2 = (1 - \gamma)\dot{M}_{12}$, we obtain

$$\frac{dR_{d2}(t)}{dt} = \lambda \left(\frac{C_{s1}}{C_{s2}}\right)\left(\frac{C_{r2}}{C_{s1}}\right) - a_{r/s}\left[R_{d2}(t) - R_{d1}(t)\right]\frac{\dot{M}_2}{M_2(t)}, \tag{54}$$

where $a_{r/s}$ is defined by

$$a_{r/s} \equiv \left(\frac{1}{1-\gamma}\right)\left(\frac{C_{s1}}{C_{s2}}\right) = \left(1 + \frac{\gamma d_{r23}}{1-\gamma}\right)\left(1 + f_2^{r/s}\right). \tag{55}$$

Because

$$\left(\frac{C_{s1}}{C_{s2}}\right)\left(\frac{C_{r2}}{C_{s1}}\right) = \left(\frac{C_{r1}}{C_{s1}}\right)\left(1 + f_2^{r/s}\right), \tag{56}$$

we obtain

$$\begin{aligned}\frac{dR_{d2}(t)}{dt} &= \lambda\left(\frac{C_{r1}}{C_{s1}}\right)\left(1 + f_2^{r/s}\right) - a_{r/s}\left[R_{d2}(t) - R_{d1}(t)\right]\frac{\dot{M}_2}{M_2(t)} \\ &\quad \times \lambda\frac{C_{r1}(0)\,e^{-\lambda t}}{C_{s1}} + \frac{C_{r1}(0)}{C_{s1}(0)} f_2^{r/s}\lambda e^{-\lambda t} - a_{r/s}\left[R_{d2}(t) - R_{d1}(t)\right]\frac{\dot{M}_2}{M_2(t)} \\ &= \frac{dR_{d1}(t)}{dt} + \frac{C_{r1}(0)}{C_{s1}(0)} f_2^{r/s}\lambda e^{-\lambda t} - a_{r/s}\left[R_{d2}(t) - R_{d1}(t)\right]\frac{\dot{M}_2}{M_2(t)},\end{aligned} \tag{57}$$

and it follows that the ratio of a daughter isotope to a stable reference isotope of the same element (with no parent) in the mantle is given by

$$R_{d2}(t) = R_{d1}(t) + \frac{N_{r1}(t)}{N_{s1}(t)} f_2^{r/s}\lambda e^{\lambda t}\int_0^t \left[\frac{M_2(\xi)}{M_2(t)}\right]^{a_{r/s}} e^{-\lambda\xi}\,d\xi \tag{58}$$

The deviations of the radiogenic isotope ratios in parts in 10^4 from the ratios in the undifferentiated reference reservoir are defined by:

$$\varepsilon^*_{dj}(t) \equiv \left[\frac{\frac{N_{dj}(t)}{N_{sj}(t)}}{\frac{N_{d1}(t)}{N_{s1}(t)}} - 1\right] 10^4. \tag{59}$$

Calculations with this model for arbitrary accretion rates are most easily done with the final equations expressing the radiogenic isotope effect in ε-values:

$$\varepsilon^*_{d2}(t) = Q^*_d(t) f_2^{r/s} e^{\lambda t} I_{a_{r/s}}(\lambda, t), \tag{60}$$

where

$$I_{a_{r/s}}(\lambda, t) \equiv \int_0^t \left[\frac{M_2(\xi)}{M_2(t)}\right]^{a_{r/s}} e^{-\lambda\xi}\,d\xi \tag{61}$$

$$Q^*_d(t) \equiv \left[10^4\lambda\left(\frac{N_{r1}(t)}{N_{d1}(t)}\right)\right]. \tag{62}$$

For an extinct nuclide system, it is better to write the Q-value on the following form:

$$Q_d^*(t) = q_d(t)\left(\frac{C_{r1}(0)}{C_{\rho 1}(0)}\right)\lambda e^{-\lambda t}, \tag{63}$$

where

$$q_d(t) = 10^4\left(\frac{C_{\rho 1}(0)}{C_{d1}(t)}\right) \cong 10^4\left(\frac{C_{\rho 1}(0)}{C_{d1}(0)}\right). \tag{64}$$

The last approximation holds well for Hf-W because $C_{d1}(t)$ only varies by a few ε-units over Earth's history. Thus, for an extinct system

$$\varepsilon_{d2}^*(t) = q_d\left(\frac{C_{r1}(0)}{C_{\rho 1}(0)}\right)\lambda f_2^{r/s} I_{a_{r/s}}(\lambda, t). \tag{65}$$

Also note that

$$\frac{\varepsilon_{d2}^*(t)}{\varepsilon_{d3}^*(t)} = \frac{f_2^{r/s}}{f_3^{r/s}}. \tag{66}$$

Thus,

$$\varepsilon_{d3}^*(t) = \frac{f_3^{r/s}\varepsilon_{d2}^*(t)}{f_2^{r/s}} = -\frac{\varepsilon_{d2}^*(t)}{f_2^{r/s}} \tag{67}$$

because $f_3^{r/s} = -1$. By using this relationship with data in Table 2, estimates of core W isotope compositions were made for Vesta, Mars, Moon, and Earth and also estimates of the W isotope compositions of silicate mantles for iron meteorite parent bodies. The W isotope composition of the core of Vesta is estimated at $\varepsilon_{W(BSE)}(0) = -3.17 \pm 0.34$. Because the initial $\varepsilon_{W(BSE)}(0)$ of the eucrite isochron is -1, this requires that the time of eruption of these basalts on the surface of Vesta postdates core formation in Vesta (Yin et al. 2002b). Core formation in Vesta must thus be substantially earlier than 3 Myr.

Note that for both Hf-W and U-Pb,

$$a_{r/s} = 1 + f_2^{r/s} \tag{68}$$

because $d_{U23} = d_{Hf23} = 0$ (i.e., U and Hf are both lithophile elements). Thus, $a_{U/Pb} = 2$ and $a_{Hf/W} = 13$.

5. RESULTS

By using the data (and parameters inferred from this data) compiled for the Hf-W chronometer in Table 2, we can evaluate various proposed scenarios for the formation history of Earth as well as other Solar System objects.

5.1. Exponential Accretion

A number of calculated accretion histories for the terrestrial planets can be approximated with an exponentially decreasing accretion rate (cf. Wetherill 1986). In this case, $\dot{M}_{accr} = \beta e^{-\alpha t}$ and the mass evolution function is

$$\frac{M_{\oplus}(\xi)}{M_{\oplus}(t)} = \frac{M_2(\xi)}{M_2(t)} = \frac{1 - e^{-\alpha\xi}}{1 - e^{-\alpha t}}, \tag{69}$$

where $0 \leq \xi \leq t$. The fractional mass of Earth ($M_{\oplus}(t)/M_{\oplus}(T_0)$) as a function of time is shown in Figure 5*a* for various values of the mean time of accretion, $\langle t \rangle$, ranging from 10 to 100 Myr. For this model, with an exponentially decreasing rate of accretion, the mean time shown is the time that is required to build ~63% of Earth's mass, and its present value is simply the inverse value of α in the equation above ($\langle t \rangle = \alpha^{-1}$; Jacobsen & Harper 1996).

For integral values (n) of $a_{r/s}$, we obtain the following expression for the integral (I_n) in the equation for the ε^*_{d2}-value:

$$I_n(\lambda, t) = \int_0^t \left(\frac{M_2(\xi)}{M_2(t)}\right)^n e^{-\lambda\xi} d\xi$$

$$= \frac{1}{1 - e^{-\alpha t}} \sum_{k=0}^{n} \frac{(-1)^k n!}{(n-k)!k!} \left[\frac{1 - e^{-(\lambda + k\alpha)t}}{\lambda + k\alpha}\right]. \tag{70}$$

Using this result for the Hf-W system in Earth [$f^{Hf/W} = 12, q_W = 1.55 \times 10^{-4}$, $(^{182}\mathrm{Hf}/^{180}\mathrm{Hf})_{T_0} = 10^{-4}$, $a_{Hf/W} = 13$], we can calculate the ε_W-evolution curves by evaluating $I_{13}(\lambda, t)$ for values of $\alpha^{-1} = \langle t \rangle$ in the range of 10 to 100 Myr, as shown in Figure 5*b*. The $\varepsilon_{W(CHUR)}$ curve for a mean time of accretion of ~11 ± 0.5 Myr gives, as shown, the best fit to the present ε_W-value for the BSE.

The present value of the integral in the expression for the ε_W-value is simply

$$I_n(\lambda, 0) = \frac{1}{\lambda} \prod_{k=1}^{n} \frac{k\alpha}{\lambda + k\alpha} = \frac{1}{\lambda} \prod_{k=1}^{n} \frac{1}{1 + (\lambda/k)\langle t \rangle}. \tag{71}$$

The parameters for the Hf-W system (Table 2) of Vesta, Mars, Moon, and Earth have been used with Equations 65 and 71 to constrain the mean time of formation of each of these bodies, as shown in Figures 6 and 7. For the range of plausible $f^{Hf/W}$-values of Vesta's mantle, one would expect $\varepsilon_W(0)$ in the range of 20 to 26, only slightly higher than its estimated $\varepsilon_W(0)$-value of 19 ± 2. The calculated curves of $\varepsilon_W(0)$ versus $\langle t \rangle$ for Vesta intersect this observed value $\langle t \rangle = 0.8 \pm 0.8$ Myr (Figure 6*a*). As discussed earlier, Mars suprisingly has two mantle sources with distinct Hf-W isotope signatures, the S source and the nakhlite-chassignite source. The calculated curves of $\varepsilon_W(0)$ versus the $\langle t \rangle$ for Mars intersect the corresponding observed values at $\langle t \rangle = 2^{+3}_{-2}$ Myr and $\langle t \rangle = 4 \pm 1$ Myr (Figure 6*b*). Both of these objects must have formed very early, close to the origin of the Solar System.

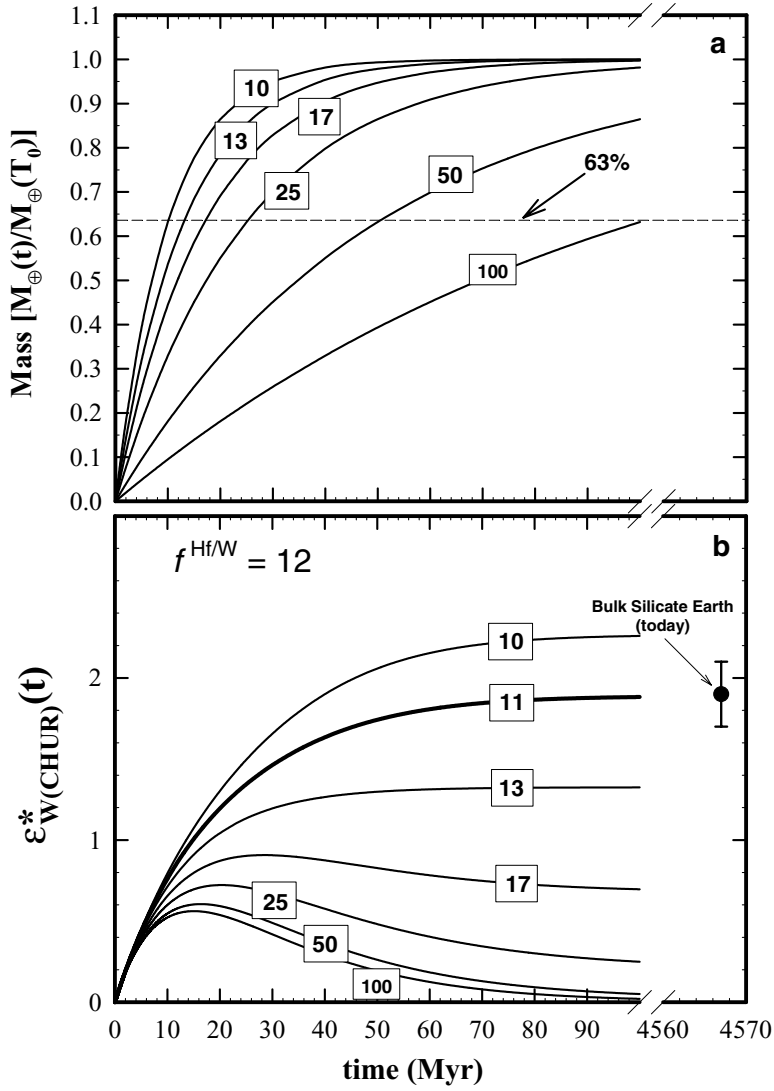

Figure 5 (*a*) The fractional mass of Earth as a function of time for a model with an exponentially decreasing rate of accretion. Growth curves are shown for various values for the mean time of accretion, $\langle t \rangle$, ranging from 10 to 100 Myr. For this model, the mean time of accretion is the time that is required to build ~63% of Earth mass. (*b*) The calculated W-isotopic evolution (ε_W) in the silicate Earth for this model. As shown, the present-day W-isotopic compositions of the BSE ($\varepsilon_W = 1.9$) is consistent with a short mean time of accretion of ~10 Myr.

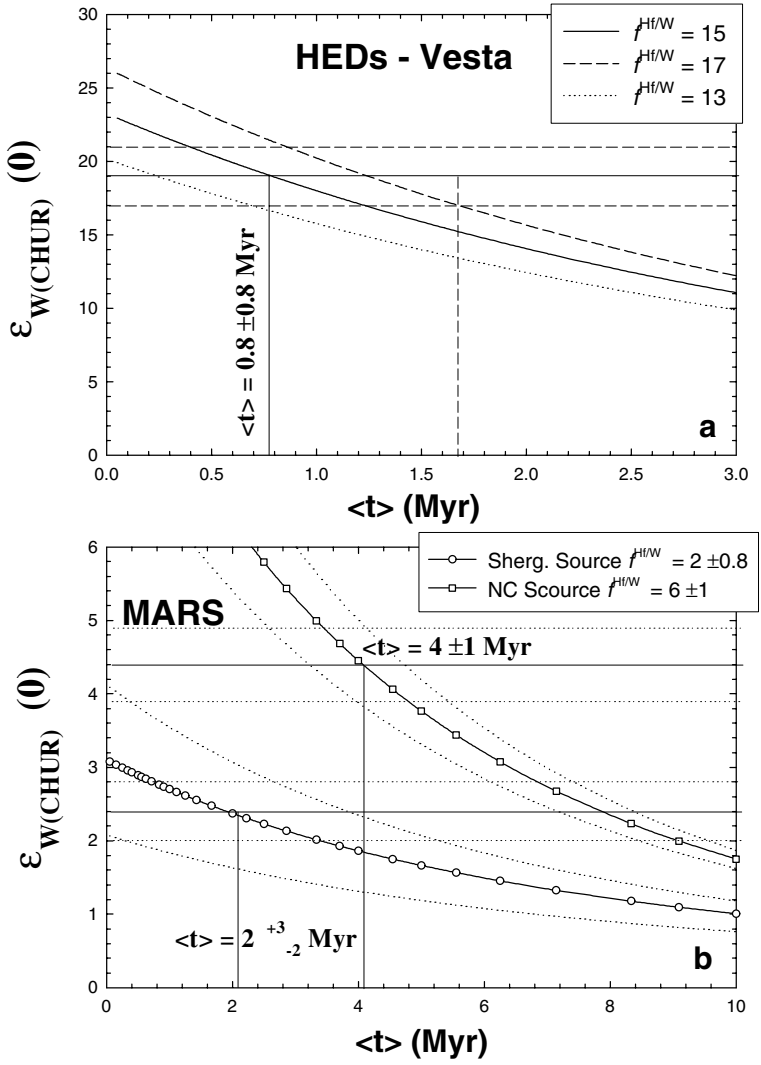

Figure 6 Present ε_W-value relative to CHUR as a function of the mean time of accretion and $f^{Hf/W}$-values assuming exponentially decreasing accretion rates. Results are shown for (*a*) Vesta and (*b*) Mars using estimates of ε_W and $f^{Hf/W}$ from Table 2.

Although the results for the two martian mantle sources are within error of each other, the S source is represented by most martian meteorite data, and the apparent later formation for the NC source could represent silicate differentiation in a magma ocean as suggested by its high ^{142}Nd value (Harper et al. 1995).

A similar treatment has been used for the Moon (Figure 7*a*). This may not be appropriate because the Moon may have formed by a giant impact (see below).

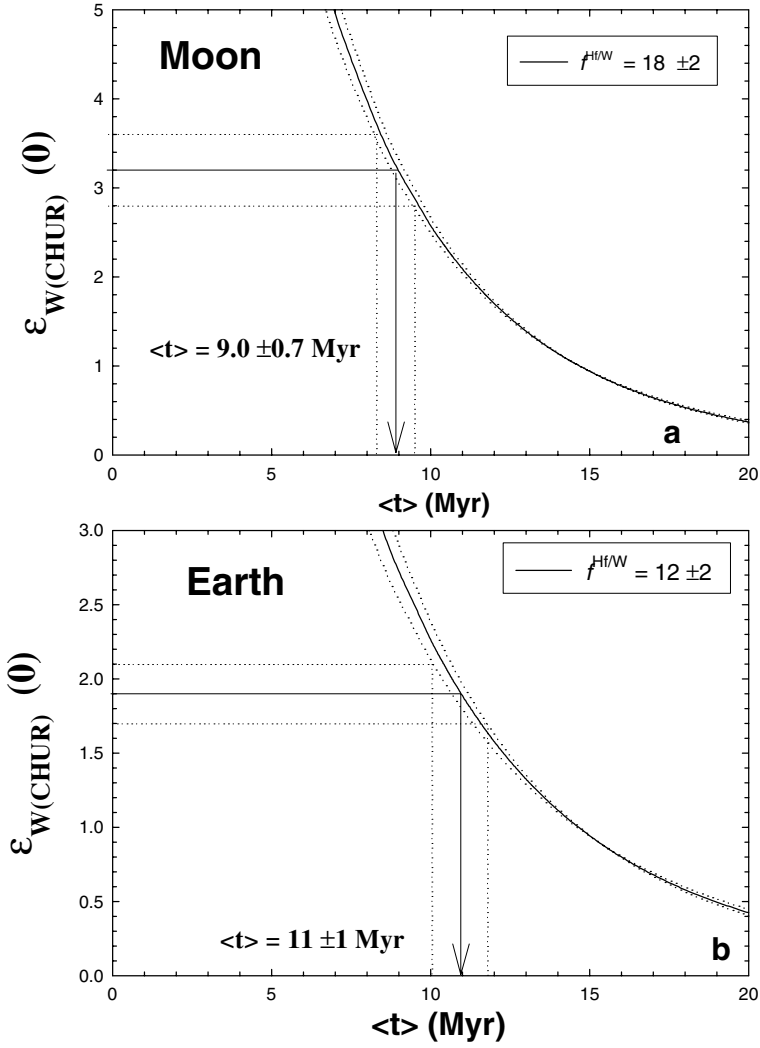

Figure 7 Present ε_W-value relative to CHUR as a function of the mean time of accretion and $f^{Hf/W}$-values assuming exponentially decreasing accretion rates. Results are shown for (*a*) the Moon and (*b*) Earth using estimates of ε_W and $f^{Hf/W}$ from Table 2.

The calculated curve of $\varepsilon_W(0)$ versus the $\langle t \rangle$ for the Moon intersect the inferred ε_W-value of the Moon at $\langle t \rangle = 9.0 \pm 0.7$ Myr. Similarly, for Earth we have $\langle t \rangle = 11 \pm 1$ Myr (Figure 7*b*) consistent with the estimate from Figure 5. The uncertainty here is a little larger than above because the intersection also takes into account a ±2 uncertainty in the $f^{Hf/W}$ value (shown by dotted curves in Figure 7).

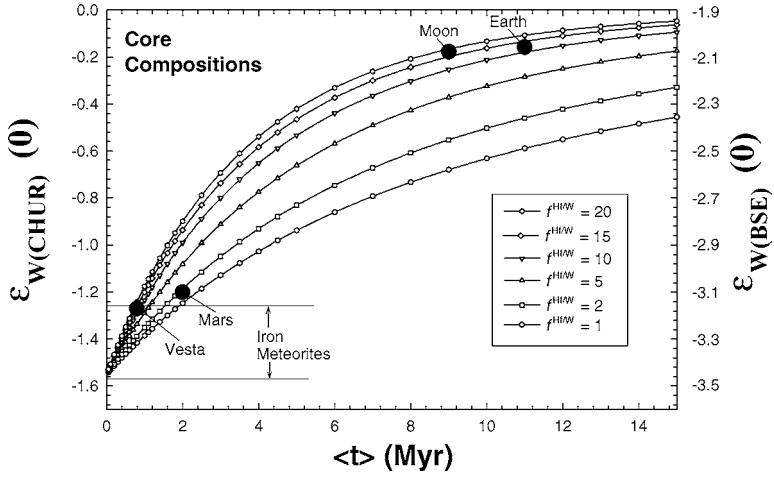

Figure 8 Estimated core compositions for Vesta, Mars, Moon, and Earth. Curves of ε_W versus $\langle t \rangle$ are shown for cores formed in parent bodies with $f^{Hf/W}$ ranging from 1 to 20.

The compositions of the cores can also be evaluated using these results and Equations 65, 67, and 71, above. The present $\varepsilon_{W(CHUR)}$ of cores are shown for $f^{Hf/W}$-values ranging from 1 to 20 and as a function of $\langle t \rangle$ (Figure 8). As can be seen for typical $f^{Hf/W}$-values of 10–20, this is a relatively sensitive chronometer. The compositions of the cores of Vesta, Mars, Earth, and Moon are shown. The range of $\varepsilon_{W(CHUR)}(0)$ in iron meteorites, the only cores measured directly, is also shown. If $f^{Hf/W} = 1$ for the mantles of iron meteorite parent bodies, then the measured range corresponds to a mean time of formation $\langle t \rangle \sim 2$ Myr. However, their $f^{Hf/W}$ values are more likely ~ 15, and if this is the case they should all have formed with a mean time of formation of less than 0.8 Myr. If the Hf/W ratio of the silicate mantles can be approximately established for the parent bodies of these iron meteorite groups, then a resolution of ± 0.1 in $\varepsilon_W(0)$ should enable a time resolution of approximately ± 0.4 Myr.

5.2. Following the Growth of a Planet by N-Body Integrations

Computer modeling of the final stage of accretion has produced many simulations of the main growth stage of Earth and the other terrestrial planets (Wetherill 1992, Chambers & Wetherill 1998, Agnor et al.1999, Chambers 2001). An example of such a history of the growth of Earth, with $\langle t \rangle = 26.7$ Myr, obtained by N-body simulation, is shown in Figure 9*a* (results from figure 13 of Agnor et al. 1999). The discrete growth events in this figure correspond to major collisions of proto-Earth with other planetary embryos or sweeping up of remaining planetesimals. The behavior of the isotopic composition (ε^*_{d2}) of the evolving silicate mantle, for

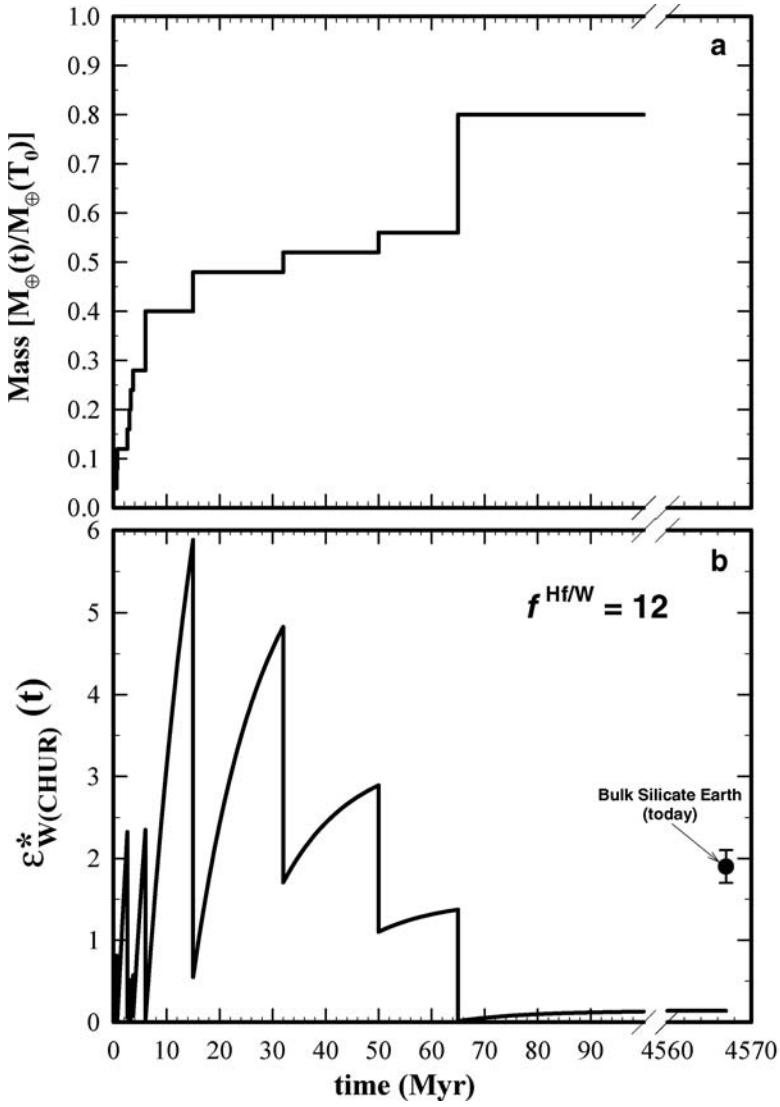

Figure 9 Growth of Earth by embryo collisions. Mass growth curve in (*a*) from Agnor et al. (1999, figure 13). The calculated ε_W-evolution shows that giant impacts always essentially eliminate the excess ^{182}W in the silicate Earth. Subsequent to ~50 Myr after the origin of the Solar System will there be insignificant recovery of the ^{182}W excess in the silicate Earth to leave it with chondritic W (Jacobsen 1999), which is clearly inconsistent with the ε_W-value of the BSE.

such a history, can be understood by differentiating Equation 65 and obtaining the following:

$$\frac{d\varepsilon^*_{d2}}{dt} = q_d(t)\left(\frac{C_{r1}(0)}{C_{\rho 1}(0)}\right)\lambda f_2^{r/s} e^{-\lambda t} - a_{r/s}\frac{\dot{M}_2}{M_2}\varepsilon^*_{d2} - 10^{-4} Q^*_d(t)\,\varepsilon^*_{d2}. \quad (72)$$

Here the last term is insignificant for the Hf-W system. For a time interval with constant mass ($\dot{M}_2 = 0$) in between collisions with planetesimals or embryos we have

$$\frac{d\varepsilon^*_{d2}}{dt} = q_d\left(\frac{C_{r1}(0)}{C_{\rho 1}(0)}\right)\lambda f_2^{r/s} e^{-\lambda t}. \quad (73)$$

The radiogenic ingrowth for a decay system with q_d effectively constant (such as Hf-W) over a time interval from t_i to t_f is thus

$$\varepsilon^*_{d2} = \varepsilon^*_{d2}(t_i) + q_d\left(\frac{C_{r1}(0)}{C_{\rho 1}(0)}\right) f_2^{r/s}[e^{-\lambda t_i} - e^{-\lambda t_f}]. \quad (74)$$

Note that because this is a stage of closed system evolution of the silicate mantle, this equation is equivalent to Equation 12. As shown for Hf/W in Figure 9*b*, the ingrowth during such stages is initially rapid but dies off with time as ^{182}Hf decays away.

Mass-growth following collisional events will cause metal saturation, consequent metal segregation, and rapid core growth on a timescale that is short compared with that for radiogenic growth. The nature of this process may in part depend on whether the impactor is already differentiated into a mantle and core. For planetesimal impacts, the impactor is largely vaporized and its mass is transported into the atmosphere and redeposited around Earth, so whether it is differentiated or not makes no difference. Simulation of giant impacts shows that for Mars-sized impactors, the mantle and core of the impactor will be completely disrupted, and individual parcels of metal from the core of the impactor will rain through the proto-Earth mantle (Canup 2004). The very high temperature that would exist under such conditions may completely dissolve all the FeNi-metal in the silicate magma ocean. Metal will be reprecipitated as Earth cools off to allow for continued core formation. Equation 72 can, for a very short interval (no decay), be simplified to

$$\frac{d\varepsilon^*_{d2}}{dt} = -a_{r/s}\frac{\dot{M}_2}{M_2}\varepsilon_{d2}, \quad (75)$$

and the difference between the initial (t_i) and final states (t_f) are given by

$$\varepsilon^*_{d2}(t_f) = \varepsilon^*_{d2}(t_i)\left(\frac{M_2(t_i)}{M_2(t_f)}\right)^{a_{r/s}}. \quad (76)$$

For impactor to proto-Earth mass ratios of 1:99, 1:19, 1:9, 2:8, and 3:7, we obtain a reduction in the isotope effect of 0.88, 0.51, 0.28, 0.055, and 0.01, respectively for

the Hf-W system ($a_{Hf/W} = 13$). The tungsten isotopic evolution corresponding to the mass growth in Figure 9*a* is shown in Figure 9*b*. It shows that for most growth steps, the ε_W-value is significantly reduced, and that it is reduced to ~0 for giant impacts; however, this scenario will not produce the observed tungsten isotopic composition of Earth's mantle ($\varepsilon_W = 1.9$). If we rescale the mass evolution in Figure 9*a* to have the final giant impact at 29 Myr rather than 65 Myr, then this will yield the observed ε_W of 1.9 for the silicate Earth and a mean time of accretion of $\langle t \rangle = 11.9$ Myr. The procedure outlined here provides a tool for direct testing of N-body simulations by using the W isotopic constraints.

5.3. Giant Impacts and the Origin of the Moon

Cameron & Ward (1976) proposed that the Moon formed by a giant impact of a Mars-sized body on Earth. Later giant impact simulations eventually led Cameron (2000) to a revised giant impact theory with an impact of a twice-Mars-sized body during accretion. However, a more exhaustive study of this problem by Canup & Asphaug (2001) concluded that the Mars-sized impact at the end of accretion is what still fits best. The Hf-W isotopic results can be used to evaluate these two contrasting suggestions. As shown in Figure 9*b*, giant impacts always reduce the ε_W in the silicate Earth to ~0, thus eliminating the excess ^{182}W. Also for giant impacts subsequent to ~50 Myr, there is insignificant recovery of the ^{182}W excess in the silicate Earth, which leaves Earth with chondritic W (Jacobsen 1999). Because the silicate Earth does not have chondritic W, we must conclude that any giant impact must have occurred substantially earlier than 50 Myr.

The growth of Earth by relatively slow accretion, followed by the addition of an impactor with a proto-Earth to impactor mass ratio of 7:3 (occurring at half the total accretion time) and then by 20% growth of Earth subsequent to the addition from the giant impact, is shown in Figure 10*a*). This mass evolution corresponds to the revised giant impact theory of Cameron (2000). The tungsten-isotopic evolution (ε_W) in the BSE corresponding to the accretion history in Figure10*a* is shown in Figure 10*b*. It was calculated using equations for exponential accretion with Equation 76 followed by closed system evolution (Equation 12), and constrained to yield the present ε_W value of the silicate Earth. This results in the giant impact at 18 Myr rather than 50 Myr, as was originally assumed by Cameron (2000). In this scenario, the ε_W is reduced from 0.75 to ~0 at 18 Myr, and following the giant impact, ε_W rises to ~1.08 and then decays to approximately 0.94 by 36 Myr, but after termination of accretion rises to 2.1 within error of the observed values, and also yields a mean time of accretion of $\langle t \rangle = 13.5$ Myr. The calculated W-isotopic evolution (ε_W) of the Moon, assuming it starts out with $\varepsilon_W \sim 0$, is also shown. This closed system W-isotopic growth for the Moon with an origin of the Moon at 18 Myr (assuming the bulk Moon $f^{Hf/W}$-value of 18) yields a present ε_W of +7, much higher than the observed value of approximately +3.

The growth of Earth by rapid exponential accretion terminated by the addition of an impactor with a proto-Earth to impactor mass ratio of 9:1 is shown in Figure 11*a*. This corresponds to the giant impact scenario favored by Canup & Asphaug (2001).

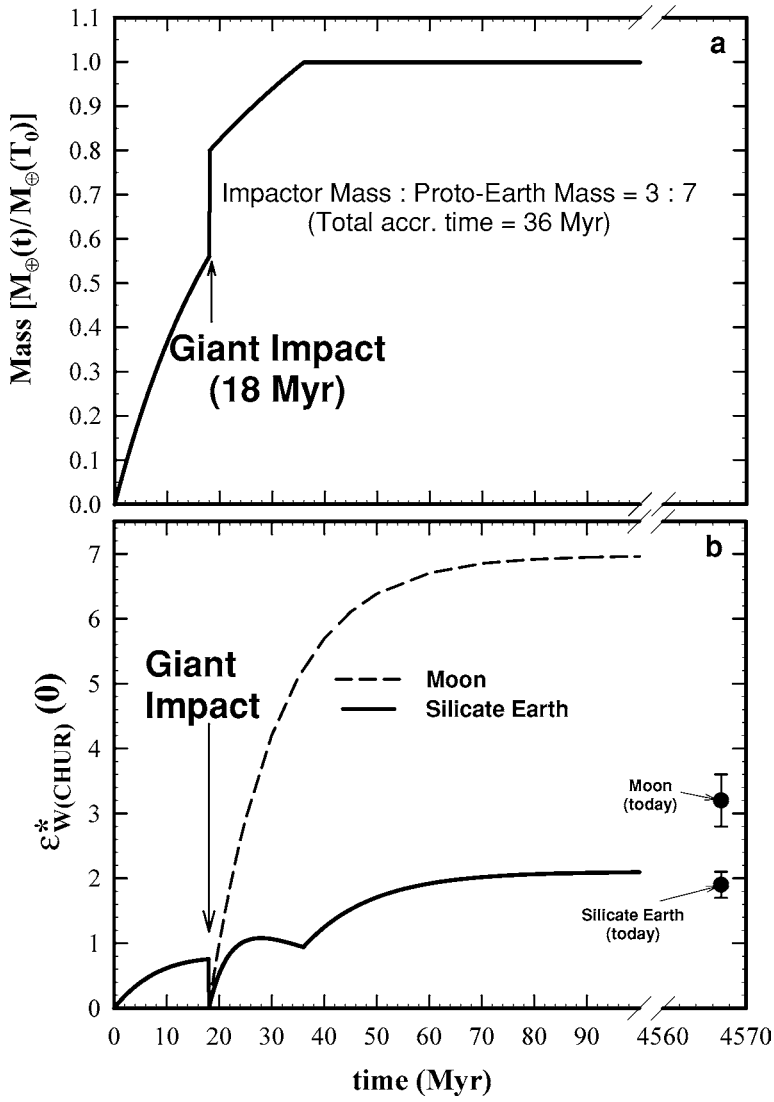

Figure 10 (*a*) Accretion with a giant impactor (proto-Earth to impactor mass ratio of 7:3) during accretion, corresponding to the revised giant impact theory of Cameron (2000). (*b*) The ε_W-evolution of the silicate Earth is constrained to give the observed present ε_W of the BSE. This yields a total timescale of 36 Myr and a giant impact at 18 Myr. However, the calculated ε_W evolution for the Moon yields a value of $\sim$+7, which is much more radiogenic than the observed value of $\sim$+3.2.

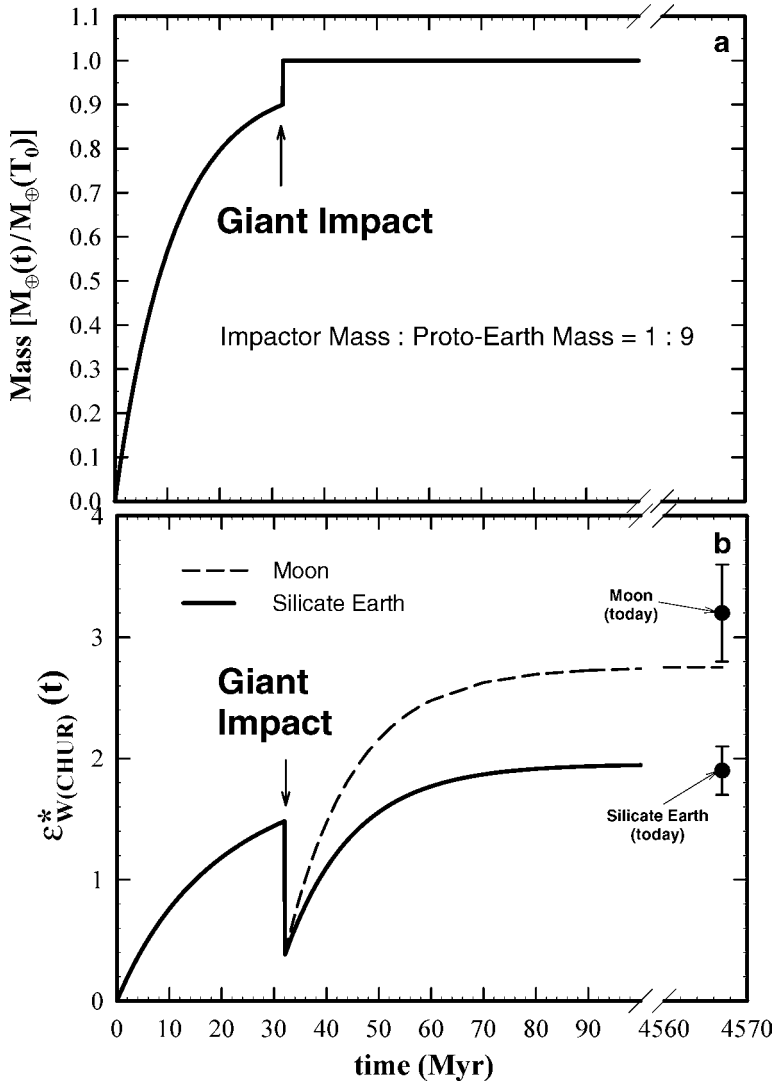

Figure 11 (*a*) Accretion followed by the addition of an impactor (proto-Earth to impactor mass ratio of 9:1) at the end of accretion, corresponding to the preferred giant impact theory of Canup & Asphaug (2001). The ε_W-evolution of the silicate Earth is constrained to give the observed present ε_W of the BSE. This yields a total timescale of 32 Myr with a giant impact at that time. For this case, the calculated ε_W evolution for the Moon yields a value of $\sim$+2.8, fairly close to the observed value of $\sim$+3.2.

The resulting tungsten-isotopic evolution (ε_W) in the BSE for the accretion history in Figure 11*a* is shown in Figure 11*b*. It was calculated using equations for exponential accretion with Equation 76 followed by closed system evolution. As shown, after termination of accretion by the giant impact at 32 Myr, ε_W is reduced to ~0.4; during subsequent closed system evolution, ε_W rises to 2.0, within error of the observed values and results in a mean time of formation of 11.5 Myr. The calculated W-isotopic evolution of the Moon assumed an origin of 32 Myr (with a $f^{Hf/W}$-value of 18) and results in ε_W of +3 similar to the observed value. Thus, this model is consistent with Hf-W isotopic systematics for both Earth and Moon.

Finally, we note that the Hf/W ratio of the lunar mantle has been estimated at $f^{Hf/W} \sim 30$ by Lee et al. (1997). If reservoirs with such high Hf/W ratios formed immediately at the time of formation, then it is possible to have the Moon form fairly late (i.e., at ~50 Myr). However, if such high Hf/W ratios are due to the formation of cumulate layers in the lunar magma ocean at a late time (~100 Myr), then the Moon must have formed prior to ~30 Myr.

5.4. Comparison with Other Model Times

Two-stage model times are readily calculated from Equation 14, and many papers on Hf-W as well as other extinct chronometers primarily discuss their results in terms of this type of model time (Lee & Halliday 1995, 1996,1997; Lee et al. 1997; Kleine et al. 2002; Schoenberg et al. 2002a). It is therefore useful to compare the two-stage model time (t_{2stage}) for extinct nuclides with the mean time of formation, $\langle t \rangle$, which is used here. From Equations 14 and 71, it follows, that for exponential accretion, we obtain the following simple relation between t_{2stage} and $\langle t \rangle$:

$$t_{2stage} = \frac{1}{\lambda} \sum_{k=1}^{n} \ln \left[1 + \left(\frac{\lambda}{k} \right) \langle t \rangle \right] \tag{77}$$

for integral values (n) of $a_{r/s}$. The results are shown in Figure 12 where the mean accretion time ($\langle t \rangle = \alpha^{-1}$) is plotted as a function of the two-stage model age for various values of $a_{r/s}$. For the Hf-W system, the difference between these two model times is strongly dependent on both the $f^{Hf/W}$-value ($a_{Hf/W} = 1 + f^{Hf/W} = 13$ for the silicate Earth) and $\langle t \rangle$. Thus for typical planetary mantle values, where $a_{Hf/W}$ is in the range 10 to 20, t_{2stage} is a factor of 2.5 to 3 larger than $\langle t \rangle$. In contrast, for an extinct system with $a_{r/s} \sim 2$, the two model times are similar.

6. DISCUSSION AND CONCLUSIONS

I have reviewed the evidence based on the Hf-W radiogenic isotope system for the processes and timescales of terrestrial planet formation. This extinct nuclide system is unique in its properties and should, in my opinion, be used as one of the primary constraints on models of planetary formation. Although other chronometers

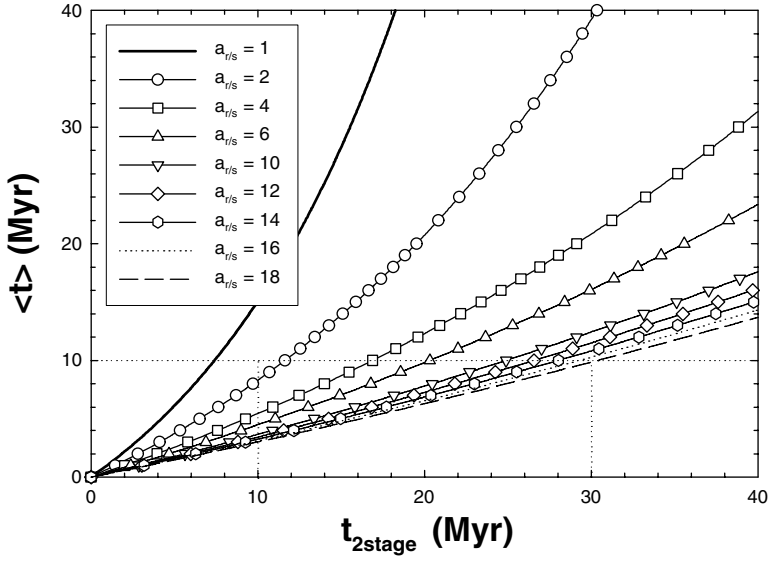

Figure 12 Comparison of the mean time of formation ($\langle t_{eq} \rangle$) and two-stage model time (t_{2stage}) for extinct nuclide chronometers as a function of the $a_{r/s}$-value. As shown, if $a_{r/s} \sim 2$, then the two model times yields about the same value. However, for a system like Hf-W, where $a_{r/s}$ is typically in the range 10–20, the two model times can be different by a factor of 3.

(U-Pb, I-Pu-Xe, etc.) may produce results that are in apparent conflict with the Hf-W system, this is because they all respond in a more complex way to Earth evolution processes (Harper & Jacobsen 1996a, Jacobsen & Harper 1996). Currently, our primary tools for understanding the formation of the terrestrial planets and extra-solar Earth-like planets are limited to (*a*) the cosmochemical record of the Solar System, (*b*) observations of circumstellar disks, and (*c*) computer simulations of terrestrial planet formation. Although computer models have been substantially improved, only a multidisciplinary approach to terrestrial planet formation is likely to lead to accurate models of planetary accretion that apply to both our Solar System as well as the formation of Earth-like planets in other planetary systems. Although direct observation of Earth-like planets around other stars is expected within the next decade, we can already observe protoplanetary disks and giant planets orbiting other stars. By understanding the formation of the terrestrial planets in our Solar System, we will be in a position to predict much about extrasolar "Earths" before they are discovered.

6.1. Planetesimal and Embryo Stage

Observations from young stellar objects show that the primary nebular dust disappears after approximately 2-3 Myr (Haisch et al. 2001), so by that time all of

the dust must be accreted into planetesimals. The evidence from computer models (Lecar & Aarseth 1986, Wetherill 1986, Canup & Agnor 2000, Ward 2000) in general supports the planetesimal hypothesis, according to which, the terrestrial planets formed by accretion of a very large number of small bodies orbiting the young Sun in a protoplanetary disk. Computer simulations suggest that runaway growth took place early (within 10^5–10^6 years) in the accretion process, when planetesimals with above average mass accreted material faster than smaller bodies and, eventually, the largest objects swept up most of the solid mass in the disk and became Moon- to Mars-sized planetary embryos (Kokubo & Ida 1998, 2000; Kortenkamp et al. 2000, 2001). This timescale is broadly compatible (considering uncertainties) with the short timescales of differentiation obtained by the Hf-W chronometry for Vesta, iron meteorite parent bodies, and Mars. One would expect, as for the asteroid belt, that accreting planetesimals in Earth's feeding zone to have both a population of undifferentiated bodies with variable volatile element depletion similar to chondrite parent bodies (CPBs), as well as differentiated bodies similar to the eucrite parent body (EPB) and iron meteorite parent bodies (IPBs). Differentiated small bodies would be expected to have suffered extensive degassing by analogy with the very low noble gas content in the eucrite metorites (cf. Miura et al. 1998). A planet accreted by coagulation of such bodies without additional gas sources would thus have very low interior gas abundances similar to those observed in eucrites. From the low gas content of the Moon and Mercury, it might be inferred that embryos up to this size are relatively gas free. However, their gas-free nature may in both cases be related to total melting after late giant impacts and gas loss after the dissipation of the nebular gas from the inner Solar System. Larger embryo's must have accreted gas, as both Mars and Earth contain much more gas than the EPB, which suggests the presence of nebular gas during part of the main planet building stage (see below).

6.2. The Main Planet Building Stage

Accretion proceeded at late stages by collisions of large (and therefore likely highly differentiated) bodies. This stage happened much more slowly and was highly stochastic. The planetary embryos collided with one another in giant impacts and swept up the remaining planetesimals. In smaller scale early impacts as well as later giant impacts (see below) by planetesimals and embryos, the impactor is largely vaporized and its mass is transported into the atmosphere and redeposited around Earth. This is followed by metal-silicate separation in a magma ocean (see Section 5.2). Computer simulations of this final stage of accretion have succeeded in producing systems containing 2–4 terrestrial planets between 0 and 2 AU from the Sun, with roughly circular and coplanar orbits (Wetherill 1992, Chambers & Wetherill 1998, Agnor et al. 1999, Chambers 2001). However, they also produce results that are incompatible with the Hf-W chronometer and various other cosmochemical constraints: (*a*) for most simulations it takes at least 10^8 years to make Earth, inconsistent with the Hf-W time of $\sim 10^7$ years (Yin et al. 2002a,b; Schoenberg et al. 2002a; Kleine et al. 2002); and (*b*) cosmochemical constraints

suggest narrow and probably separate feeding zones for each of the terrestrial planets (cf. Taylor 1999), whereas computer models suggest much wider feeding zones (Chambers 2001). Also, a number of features of the terrestrial planet computer model systems generally differ from the real terrestrial planets in several ways (cf. Chambers 2001): (*a*) orbits from simulations are more eccentric and inclined than those of Earth and Venus, (*b*) Mars- and Mercury-like planets are rarely produced in the simulations, and (*c*) the high concentration of mass in the region occupied by Venus and Earth is not reproduced in the simulations. Thus, there are many remaining problems to solve before we have a good theory for the final stage of terrestrial planet formation. It is important to note that the noble gas evidence suggests that the Earth had a substantial solar composition atmosphere during most of the main planet building stage (Harper & Jacobsen 1996b). Thus, initially accretion of Earth's atmosphere is directly from the nebular gas present in a disk with embryos and planetesimals. Such proto-atmosphere accretion by gravitational capture appears to be possible for growth of bodies of Mars to Earth size, and the nebula must retain gas at this stage. Part of the gas budget in Earth's interior is established by solution of noble gases from the proto-atmospheres into a high temperature magma ocean (Harper & Jacobsen1996b). It is therefore important to include the presence of nebular gas during this stage in future computer models.

6.3. Giant Impacts and Mergers

Earth probably acquired many of its orbital characteristics as well as its Moon during a late accretion phase as a result of at least one giant impact. In this connection it is important to define clearly what is implied by the term giant impact compared to proto-planetary mergers late in the accretion process. Harper & Jacobsen (1996a) discussed the issue of whether there should exist a real scale changeover from explosive disruption of the impactor during the giant impact to a core-penetration-merger mode of accretion as the impactor to planet-size ratio is increased. This was because the smooth particle hydrodynamic (SPH) modeling by Cameron & Benz (1991) suggested that cores in giant impacts may merge penetratively without mixing and equilibrate with their mantles. However, as discussed earlier, from the recent higher resolution SPH work of Canup (2004), it appears that differentiation following a Mars-sized giant impactor will follow the general model discussed here (impactor metal reequilibrated in the magma ocean) and not a core-penetrative mode. A giant impact may be defined for Earth as accretion of a Moon to at least a Mars-sized body ($\sim$1–10% of Earth's mass).

A merger may be defined as a larger event involving coalescence of two differentiated bodies, where the mantle sand cores are merged without any equilibration (impactor to proto-Earth mass ratio possibly in the range of at least $>1/9$ and ≤ 1). If a core-core merger were to occur without significant equilibration, then W isotopes would record age information only on the growth of the premerged objects. In the simple case of twin differentiated embryos with identical mantle

$f^{Hf/W}$-values, the W isotope composition would record the average accretion of the two objects, and no information on the chronology of the merger would be recorded. It is, however, possible that two-body mergers might lead to sufficiently high temperatures in the interior of Earth to cause complete rehomogenization of the metal and silicate liquids. Then, upon cooling, the metal core is reprecipitated and the Hf-W chronology of accretion reduces to the simple two-stage case and determines only the time of the merger. Thus, the question of whether such a merger process is feasible needs to be addressed by further computer modeling.

6.4. Other Views

It is now clear that all of the original Hf-W evidence for formation of the Moon and Earth's core at ~50–60 Myr after Solar System formation was incorrect. First, Lee et al. (1997) reported W isotope variations in lunar samples that correlated with Hf/W ratios, and they interpreted these data to define a fossil Hf-W isochron for the Moon yielding a time of formation of 54^{+7}_{-5} Myr. They later (Lee et al. 2002) recognized that the variable W isotope ratios were due to neutron capture effects rather than decay from ^{182}Hf, and that this age estimate was therefore invalid. Second, on the basis of incorrect Hf-W measurements of chondrites, Lee & Halliday (1995, 1996) argued that the age of the Earth's core was ~60 Myr and that this was consistent with a U-Pb age for Earth based on estimates of the average Pb isotope composition in the silicate Earth. Although the U-Th-Pb system can be construed to give such a late formation age of Earth (cf. Galer & Goldstein 1996), this is only one of many equally likely interpretations. First of all, the U-Th-Pb system did not primarily fractionate by core formation but by volatile element depletion in Earth. Also, it is further affected by mantle-crust evolution. In contrast, none of these processes affected the Hf-W system (Harper & Jacobsen 1996a, Jacobsen & Harper 1996, Jacobsen et al. 2004).

Halliday (2004) has recently argued that by having the Moon-forming impact occur primarily by the merger process described above, it is still possible to have the end of Earth's accretion and the formation of the Moon at ~50–60 Myr be consistent with the Hf-W isotopic constraints. He argues that for this to occur, a Moon-forming impactor the size of Mars is needed, and approximately 4% of this impactor's core is required to equilibrate with the proto-Earth mantle, whereas 96% is directly merged with the proto-Earth's core. It is also required that the impactor as well as the proto-Earth have $f^{Hf/W}$-values of ~3, and that the silicate portions of Earth and the Moon acquired their high $f^{Hf/W}$-values of 12 and 18 by changing from oxidized mantles for proto-Earth and its impactor to reduced mantles (and consequent additional metal segregation) following the giant impact. Such a model is inconsistent with the most recent and highest resolution SPH simulation of the Earth-Moon system following a Mars-sized giant impact (Canup 2004), as it does not show a direct core-core merger. As stated above, this issue of the scale of equilibration of the cores of impactors with a magma ocean needs further investigation by computer modeling of the process. Furthermore, we need

better estimates of the physical conditions prevailing in the magma ocean during the core separation process and a better determination of the equilibrium partitioning of W and other siderophile elements between metal and silicate for the appropriate physical and chemical parameters.

6.5. Conclusions

The Hf-W decay system is the best chronometer we have for understanding the main stage of terrestrial planet building. Earth has a radiogenic W-isotopic composition as compared to chondrites, demonstrating that it formed while ^{182}Hf (half-life 9 Myr) was extant in Earth and decaying to ^{182}W.

I have shown that simple analytic solutions can be obtained for the radiogenic isotope effect produced in the silicate mantle according to the standard magma ocean model of core segregation during accretion. Using this model for the Hf-W chronometer implies that Earth underwent early and rapid accretion and core formation, with most of the accumulation occurring in ~10 Myr, and concluding approximately 30 Myr after the origin of the Solar System.

The Hf-W data for lunar samples can be reconciled with a major Moon-forming impact that terminated the terrestrial accretion process ~30 Myr after the origin of the Solar System. The W isotope data is satisfactorily modeled with a Mars-sized impactor on proto-Earth (proto-Earth to impactor ratio of 9:1) to form the Moon at ~30 Myr. To improve our estimate of the age of the Moon, we need more and better W isotope data for lunar samples as well as an improved understanding of how to use this data for Hf-W chronology.

ACKNOWLEDGMENTS

This study was supported by the NASA Cosmochemistry (grant # NNG04GG06G) and Origins of Solar Systems (grant # NAG5-13164) programs.

The *Annual Review of Earth and Planetary Science* is online at http://earth.annualreviews.org

LITERATURE CITED

Agnor CB, Canup RM, Levison HF. 1999. On the character and consequences of large impacts in the late stage of terrestrial planet formation. *Icarus* 142:219–37

Amelin Y, Krot AN, Hutcheon ID, Ulyanov AA. 2002. Lead isotopic ages of chondrules and calcium-aluminum—rich inclusions. *Science* 297:1678–83

Cameron AGW. 2000. High-resolution simulations of the giant impact. See Canup & Righter 2000, pp. 133–44

Cameron AGW, Benz W. 1991. The origin of the moon and the single impact hypothesis. IV. *Icarus* 92:204–16

Cameron AGW, Ward WR. 1976. The Origin of the Moon. *Proc. Lunar Planet. Sci. Conf.* 7:120–22

Canup RM. 2004. Simulations of a late lunar-forming impact. *Icarus* 168:433–56

Canup RM, Agnor CB. 2000. Accretion of the terrestrial planets and the Earth-Moon system. See Canup & Righter 2000, pp. 113–29

Canup RM, Asphaug E. 2001. Origin of the Moon in a giant impact near the end of the Earth's formation. *Nature* 412:708–12

Canup RM, Righter K, eds. 2000. *Origin of the Earth and Moon.* Tucson: Univ. Ariz. Press. 555 pp.

Chambers JE. 2001. Making more terrestrial planets. *Icarus* 152:205–24

Chambers JE, Wetherill GW. 1998. Making the terrestrial planets: NBody integrations of planetary embryos in three dimensions. *Icarus* 136:304–27

Drake MJ, Righter K. 2002. Determining the composition of the Earth. *Nature* 416:39–44

Foley CN, Wadhwa M, Borg L, Janney PE. 2004. The differentiation history of mantle reservoirs on Mars from W and Nd isotopic compositions of SNC meteorites. *Lunar Planet. Sci.* 35:A1879. LPI, Houston (CD-ROM)

Foley CN, Wadhwa M, Janney PE. 2003. Tungsten Isotopic Composition of the SNC Meteorite Los Angeles: Further Implications for Early Differentiation History of Mars. *Lunar Planet. Sci.* 34:A2217. LPI, Houston (CD-ROM)

Galer SJG, Goldstein SL. 1996. Influence of accretion on lead in the Earth. In *Isotopic Studies of Crust-Mantle Evolution*, ed. AR Basu, SR Hart, pp. 75–98. Washington, DC: AGU

Gessmann CK, Rubie DC. 2000. The origin of the depletions of V, Cr and Mn in the mantles of the Earth and Moon. *Earth Planet. Sci. Lett.* 184:95–107

Haisch KE, Lada EA, Lada CJ. 2001. Disk frequencies and lifetimes in young clusters. *Astrophys. J. Lett*. 553:L153–56

Halliday AN. 2004. Mixing, volatile loss and compositional change during impact-driven accretion of the Earth. *Nature* 427:505–9

Halliday AN, Lee DC, Jacobsen SB. 2000. Tungsten isotopes, the timing of metal-silicate fractionation, and the origin of the Earth and Moon. See Canup & Righter 2000, pp. 45–62

Harper CL, Jacobsen SB. 1994a. Investigations of the ^{182}Hf-^{182}W systematics. *Lunar Planet. Sci*. 25:509. LPI, Houston

Harper CL, Jacobsen SB. 1994b. Accretion chronology of the inner solar system: Isotopic constraints. *Meteoritics* 29:471

Harper CL, Jacobsen SB. 1996a. Evidence for ^{182}Hf in the early solar system and constraints on the timescale of terrestrial core formation. *Geochim. Cosmochim. Acta* 60:1131–53

Harper CL, Jacobsen SB. 1996b. Noble gases and Earth's accretion. *Science* 273:1814–18

Harper CL, Nyquist LE, Bansal B, Wiesmann H, Shih CY. 1995. Rapid accretion and early differentiation of Mars indicated by ^{142}Nd/^{144}Nd in SNC meteorites. *Science* 267:213–17

Harper CL, Volkening J, Heumann KG, Shih CY, Wiesmann H. 1991. ^{182}Hf-^{182}W: new cosmochronometric constraints on terrestrial accretion, core formation, the astrophysical site of the r-process, and the origin of the solar system. *Lunar Planet. Sci.* 22:515–16. LPI, Houston

Horan MF, Smoliar MI, Walker RJ. 1998. ^{182}W and ^{187}Re-^{187}Os systematics of iron meteorites: chronology for melting, differentiation, and crystallization in asteroids. *Geochim. Cosmochim. Acta* 62:545–54

Jacobsen SB. 1988. Isotopic and chemical constraints on mantle-crust evolution. *Geochim. Cosmochim. Acta* 52:1341–50

Jacobsen SB. 1999. Accretion and core formation models based on extinct radionuclides. *Lunar Planet. Sci.* 30:A1978. LPI, Houston (CD-ROM)

Jacobsen SB, Harper CL. 1996. Accretion and early differentiation history of the Earth based on extinct radionuclides. In *Earth Processes: Reading the Isotope Code*, ed. A Basu, S Hart, Geophys. Monogr. 95:47–74. Washington, DC: AGU. 437 pp.

Jacobsen SB, Wasserburg GJ. 1979. The mean age of mantle and crust reservoirs. *J. Geophys. Res.* 84:7411–27

Jacobsen SB, Yin QZ. 1998. W isotope variations and the time of formation of asteroidal cores and the Earth's core. *Lunar Planet. Sci.* 29:1852–53. LPI, Houston (CD-ROM)

Jacobsen SB, Yin QZ, Petaev MI. 2004. On the problem of metal-silicate equilibration

during planet formation: significance for Hf-W chronometry. *Lunar Planet. Sci.* 35: A1638. LPI, Houston (CD-ROM)

Kleine T, Münker C, Mezger K, Palme H. 2002. Rapid accretion and early core formation on asteroids and the terrestrial planets from Hf-W chronometry. *Nature* 418:952–55

Kokubo E, Ida S. 1998. Oligarchic growth of protoplanets. *Icarus* 131:171–78

Kokubo E, Ida S. 2000. Formation of protoplanets from planetesimals in the solar nebula. *Icarus* 143:15–27

Kortenkamp SJ, Kokubo E, Weidenschilling SJ. 2000. Formation of planetary embryos. See Canup & Righter 2000, pp. 85–100

Kortenkamp SJ, Wetherill GW, Inaba S. 2001. Runaway growth of planetary embryos facilitated by massive bodies in a protoplanetary disk. *Science* 293:1127–29

Lecar M, Aarseth SJ. 1986. A numerical simulation of the formation of the terrestrial planets. *Astrophys. J.* 305:564–79

Lee DC, Halliday AN. 1995. Hafnium-tungsten chronometry and the timing of terrestrial core formation. *Nature* 378:771–74

Lee DC, Halliday AN. 1996. Hf-W isotopic evidence for rapid accretion and differentiation in the early solar system. *Science* 274:1876–79

Lee DC, Halliday AN. 1997. Core formation on Mars and differentiated asteroids. *Nature* 388:854–57

Lee DC, Halliday AN. 2000a. Hf-W internal isochrons for ordinary chondrites and the initial $^{182}Hf/^{180}Hf$ of the solar system. *Chem. Geol*. 169:35–43

Lee DC, Halliday AN. 2000b. Accretion of primitive planetesimals: Hf-W isotopic evidence from enstatite chondrites. *Science* 288:1629–31

Lee DC, Halliday AN, Leya I, Wieler R, Wiechert U. 2002. Cosmogenic tungsten and the origin and earliest differentiation of the Moon. *Earth Planet. Sci. Lett*. 198:267–74

Lee DC, Halliday AN, Snyder GA, Taylor LA. 1997. Age and origin of the Moon. *Science* 278:1098–103

Lodders K. 1998. A survey of shergottite, nakhlite and chassigny meteorites whole-rock compositions. *Meteor. Planet. Sci.* 33: A183–90

Lugmair GW, Shukolyukov A. 1998. Early solar system timescales according to ^{53}Mn-^{53}Cr systematics. *Geochim. Cosmochim. Acta* 62: 2863–86

Miura YN, Nagao K, Sugiura N, Fujitani T, Warren PH. 1998. Noble gases, ^{81}Kr-Kr exposure ages and ^{244}Pu-Xe ages of six eucrites, Béba, Binda, Camel Donga, Juvinas, Millbillillie, and Stannern. *Geochim. Cosmochim. Acta* 62:2369–87

Nyquist LE, Reese Y, Wiesmann H, Shih CY, Takeda H. 2001. Live ^{53}Mn and ^{26}Al in an unique cumulate eucrite with very calcic feldspar (An∼98). *Meteor. Planet. Sci.* 36:A151–52

Palme H, Rammensee W. 1981. The significance of W in planetary differentiation processes: Evidence from new data on eucrites. *Proc. Lunar Planet. Sci. Conf*. 12B:949–64

Petaev MI, Jacobsen SB. 2004. Differentiation of metal-rich meteoritic parent bodies. I. Measurement of PGEs, Re, Mo, W and Au in meteoritic Fe-Ni metal. *Meteor. Planet. Sci*. 39:1685–97

Quitté G, Birck JL. 2004. Tungsten isotopes in eucrites revisited and the initial $^{182}Hf/^{180}Hf$ of the solar system based on iron meteorite data. *Earth Planet. Sci. Lett.* 219:201–7

Quitté G, Birck JL, Allègre CJ. 2000. ^{182}Hf-^{182}W systematics in eucrites: the puzzle of iron segregation in the early solar system. *Earth Planet. Sci. Lett*. 184:83–94

Rammensee W, Wänke H. 1977. On the partition coefficient of tungsten between metal and silicate and its bearing on the origin of the moon. *Proc. Lunar Sci. Conf*. 8:399–409

Righter K, Drake MJ. 1996. Core formation in Earth's Moon, Mars, and Vesta. *Icarus* 124:513–29

Righter K, Drake MJ. 1997. Metal-silicate equilibrium in a homogeneously accreting earth:

new results for Re. *Earth Planet. Sci. Lett.* 146:541–53

Righter K, Drake MJ. 1999. Effect of water on metal-silicate partitioning of siderophile elements: a high pressure and temperature terrestrial magma ocean and core formation. *Earth Planet. Sci. Lett.* 171:383–99

Righter K, Drake MJ. 2000. Metal/silicate equilibrium in the early Earth—new constraints from the volatile moderately siderophile elements Ga, Cu, P, and Sn. *Geochim. Cosmochim. Acta* 64:3581–97

Righter K, Shearer CK. 2003. Magmatic fractionation of Hf and W: Constraints on the timing of core formation and differentiation in the Moon and Mars. *Geochim. Cosmochim. Acta* 67:2497–507

Rubie DC, Melosh HJ, Reid JE, Liebske C, Righter K. 2003. Mechanisms of metal-silicate equilibration in the terrestrial magma ocean. *Earth Planet. Sci. Lett.* 205:239–55

Ruzicka A, Snyder GA, Taylor LA. 1997. Vesta as the howardite, eucrite and diogenite parent body: implications for the size of a core and for large-scale differentiation. *Meteor. Planet. Sci.* 32:825–40

Schersten A, Elliott T, Hawkesworth C, Norman M. 2004. Tungsten isotope evidence that mantle plumes contain no contribution from the Earth's core. *Nature* 427:234–37

Schoenberg R, Kamber BS, Collerson KD, Eugster O. 2002a. New W-isotope evidence for rapid terrestrial accretion and very early core formation. *Geochim. Cosmochim. Acta* 66:3151–60

Schoenberg R, Kamber BS, Collerson KD, Moorbath S. 2002b. Tungsten isotope evidence from 3.8-Gyr metamorphosed sediments for early meteorite bombardment of the Earth. *Nature* 418:403–5

Srinivasan G, Papanastassiou DA, Wasserburg GJ, Bhandari N, Goswami JN. 2000. Re-examination of ^{26}Al-^{26}Mg systematics in the Piplia Kalan eucrite. *Lunar Planet. Sci.* 31:A1795. LPI, Houston (CD-ROM)

Stegman DR, Jellinek AM, Zatman SA, Baumgardnerk JR, Richards MA. 2003. An early lunar core dynamo driven by thermochemical mantle convection. *Nature* 421:143–46

Taylor SR. 1992. *Solar System Evolution: A New Perspective: An Inquiry Into the Chemical Composition, Origin, and Evolution of the Solar System.* Cambridge, MA: Cambridge Univ. Press. 307 pp.

Taylor SR. 1999. Leonard award address—On the difficulties of making Earth-like planets. *Meteor. Planet. Sci.* 34:317–30

Treiman AH, Drake MJ, Janssens MJ, Wolf R, Ebihara M. 1986. Core formation in the earth and shergottite parent body (SPB)—Chemical evidence from basalts. *Geochim. Cosmochim. Acta* 50:1071–91

Walter MJ, Newsom HE, Ertel W, Holzheid A. 2000. Siderophile elements in the Earth and Moon: metal/silicate partitioning and implications for core formation. See Canup & Righter 2000, pp. 265–89

Ward WR. 2000. On planetesimal formation: the role of collective particle behavior. See Canup & Righter 2000, pp. 75–84

Wasserburg GJ, Busso M, Gallino R. 1996. Abundances of actinides and short-lived non-actinides in the interstellar medium: Diverse supernova sources for the r-processes *Astrophys. J. Lett.* 466:L109

Wetherill GW. 1986. Accumulation of the terrestrial planets and implications concerning lunar origin. In *Origin of the Moon*, ed. WK Hartmann, RJ Phillips, GJ Taylor, pp. 519–50. Houston: Lunar Planet. Inst.

Wetherill GW. 1992. An alternative model for the formation of the asteroids. *Icarus* 100:307–25

Yin QZ, Jacobsen SB. 2003. The initial ^{182}W/^{183}W and ^{182}Hf/^{180}Hf of the solar system and a consistent chronology with Pb-Pb ages. *Lunar Planet. Sci.* 34:A1857. LPI, Houston (CD-ROM)

Yin QZ, Jacobsen SB, Wasserburg GJ. 2003. Cautionary notes on cosmogenic ^{182}W and other nuclei in lunar samples. *Lunar Planet. Sci.* 34:A1510. LPI, Houston (CD-ROM)

Yin QZ, Jacobsen SB, Yamashita K, Blichert-Toft J, Télouk P, Albarède F. 2002a. New

Hf-W data that are consistent with Mn-Cr chronology: implications for early solar system evolution. *Lunar Planet. Sci*. 33:A1700. LPI, Houston (CD-ROM)

Yin QZ, Jacobsen SB, Yamashita K, Blichert-Toft J, Télouk P, Albarède F. 2002b. A short timescale for terrestrial planet formation from Hf-W chronometry of meteorites. *Nature* 418:949–52

Yin QZ, Yamashita K, Jacobsen SB. 1999. Investigating the timescale of metal-silicate (Core-Mantle) differentiation using Hf-W and Tc-Mo extinct chronometers. *Lunar Planet. Sci.* 30:A2049. LPI, Houston (CD-ROM)

Annual Review of Earth and Planetary Sciences
Volume 33, 2005

CONTENTS